HUMAN OCCUPANCY DETECTION VIA PASSIVE COGNITIVE RADIO AND SIGNATURE SYNTHESIS

by

BING LIU

A thesis submitted in partial fulfillment of the
requirements for the degree of

MASTER OF SCINECE IN ENGINEERING

2020

Oakland University
Rochester, Michigan

Thesis Advisory Committee:

Jia Li, Ph.D., Chair
Daniel Aloi, Ph.D.
Shadi Alawneh, Ph.D.

ACKNOWLEDGMENTS

It has been two years since I first started my master program at Oakland University, and it has been an incredible experience.

I would like to share my gratefulness with those who helped me to achieve my academic and research goals. I would like to first thank my advisor, Dr. Jia Li, for her rich knowledge, high standard of academic requirement, candid advice and support of my research work. I can always get the guidance needed from her expertise on digital signal processing, machine learning and mathematics. The time we spent together to review the source code line by line, the delegated attitude to collect experimental data personally, every word in the paper she edited and countless help she provided, made my journey so joyful.

I would like to acknowledge my thesis committee members, Dr. Daniel N. Aloi, and Dr. Shadi Alawneh for their advices during my master study and research.

I would also like to express my gratitude to my classmate Asad Vakil for his help on my English and presentation, and Huaizheng Mu for data collection. The expertise from Dr. Erik Blasch, Dr. Robert Ewing, and Dr. Xiaoping Shen also made significant impact of my research projects. Finally, I am grateful to my parents. They always encourage me to pursue my dream regardless how far away I am from them.

This research is supported by AFOSR grant FA9550-18-1-0287.

Bing Liu

ABSTRACT

HUMAN OCCUPANCY DETECTION VIA PASSIVE COGNITIVE RADIO AND SIGNATURE SYNTHESIS

by

Bing Liu

Adviser: Jia Li, Ph.D.

Human occupancy detection (HOD) in an enclosed space via passive radio frequency (RF) data is a new and challenging research area because a human subject cannot easily be detected due to spectrum variation. We provide a complete, low-cost, and eco-friendly HOD solution via passive RF data through deep learning initially. The system can accurately estimate the human occupancy status and the efficiency is improved significantly through cognitive radio (CR) and adaptive sensing technology. Moreover, our trained RF human signatures generative adversarial network (GAN) (HSGAN) model is capable of synthesizing passive human RF signatures given the baseline spectrum of the environment measured without human occupancy. This study compensates the deficiencies of the exiting HOD technologies in an innovative and effective way. Using only passive RF signals, the crowed wireless environment is protected, and the privacy is not a concern. The solution can be applied almost anywhere as it does not dependent on specific types of wireless signals. The robustness is ensured by the awareness of its surrounding RF environment and the adaption in an unknown spectrum is achieved through its prediction ability.

TABLE OF CONTENTS

TABLE OF CONTENTS—Continued

TABLE OF CONTENTS—Continued

LIST OF TABLES

LIST OF FIGURES

LIST OF ABBREVIATIONS

HOD	Human occupancy detection
RF	Radio frequency
CNN	Convolution neural network
CR	Cognitive radio
SDR	Software defined radio
GAN	Generative adversarial network
HSGAN	Human signatures generative adversarial network
CRhodora	Cognitive radio human occupancy detection over radio frequency analysis
PCA	Principal component analysis
RFE-LR	Recursive feature elimination with logistic regression
ML	Machine learning
SVM	Support vector machine
SVM	K-nearest neighbors
DT	Decision tree
SGD	Stochastic gradient descent
RNN	Residual neural network

CHAPTER ONE

INTRODUCTION

1.1 Problem Statement

The field of human detection has many important applications, ranging from autonomous vehicles safety [1], smart building surveillance [2], and site security [3], to critical disaster relief operations. Even in less extreme applications, such as assisted living, hospitals, or smart homes, simply detecting the presence of a person is almost always the first step to any monitoring system. Human detection technology increases the efficiency of these systems, which can be lifesaving in many situations. Many solutions have been developed to solve the problem of human detection. The existing human occupancy sensing modalities include a visual camera [4], as well as lidar [5], radar [6], [7], infrared [8], and ultrasonic sensors [9]. These modalities all have their own individual strengths and weaknesses. Cameras, for example, are capable of providing detailed feature information, which is suitable for human subject identification and tracking, but can be restricted by factors such as lighting and perspective. Optical modalities such as cameras can be considered invasive and may generate privacy concerns. Lidar and radar systems are expensive, and both require signal emitters. The existing wireless systems can be interfered by the actively emitted signals. The installation angle and position are very important factors that must be considered when installing human detection devices such as infrared, ultrasonic sensors, lidar and radar. These modalities are prone to being physically obstructed or jammed. Therefore, it will be beneficial to develop a non-polluting, passive, and low-priced solution to human occupancy detection (HOD). In order to composite the existing HOD technologies, this article proposes a HOD system via passive RF data through deep learning in the enclosed spaces.

1.2 Proposed Solution

A complete HOD solution and investigation via passive RF data in the enclosed spaces is proposed in this thesis and implemented in three phases.

1.2.1 Phase One

We explore feasibility of identifying the presence of one or more people inside an enclosed space using passive radio frequency (RF) signals via deep learning neural network. The system works as following: (1) a software defined radio (SDR) collects passive RF wireless signals from surrounding environment in the enclosed spaces by scanning from its lowest frequency to its highest frequency; (2) labels are assigned to RF raw data automatically during data collection; (3) raw data is extracted from the a certain number of manually selected frequency bands. (4) a convolution neural network (CNN) model is trained with the extracted frequency bands raw data and corresponding labels; (4) the trained CNN model estimates the human occupancy status using the extracted frequency bands raw data which is unsee during the training process. The experimental results prove that the idea of HOD via deep learning of passive RF data is feasible by CNN’s very high accuracy at different locations of interest such as the residential rooms and the office.

1.2.2 Phase Two

The system prosed in the initial phase can only work in the fixed location, significant amount of training data is required to build the CNN model and manually selecting frequency bands lacks flexibility and efficiency. In order to build a more efficient and flexible real time HOD system, dynamic bands selection and online training methodologies are adopted in this phase. An advanced cognitive radio (CR) HOD over RF analysis (CRhodora) system is developed accordingly: (1) the system dynamically reconfigures a CR to collect RF frequency signals at different places of interest; (2) principal component analysis (PCA) and recursive feature elimination with logistic regression (RFE-LR) algorithms are applied to find the frequency bands sensitive to human occupancy when the baseline spectrum changes with locations; (3) with the dynamically collected passive RF signals, four machine learning (ML) classifiers are applied to detect human occupancy including support vector machine (SVM), k-nearest neighbors (KNN), decision tree (DT), and linear SVM with stochastic gradient descent (SGD) training; (4) finally, the trained classifier is used for HOD in real time through online training strategy. The experimental results show that the proposed system can accurately detect human subjects not only in residential rooms but also in commercial vehicles, which demonstrates passive CR is a viable technique for HOD. More specifically, the RFE-LR with SGD achieves the best results with a limited number of frequency bands. The proposed adaptive spectrum sensing method has not only enabled robust detection performance in various environments, but also improved the efficiency of the CR system in terms of speed and power consumption.

1.2.3 Phase Three

The wireless environment can be easily interfered by jamming signals or by replaying recorded samples. Hence, the knowledge of the RF environment is a critical aspect of a passive RF signals-based security monitoring system. Instead of retraining detectors with newly collected data, future systems should adapt to a new environment by predicting the RF signatures with human occupancy given the baseline spectrum of the environment measured without human occupancy. Synthesizing RF signatures of human occupancy is a challenging research area due to the lack of prior knowledge of how a human body alters the RF data. A human RF signatures generation system via generative adversarial networks (GAN) is proposed in this phase to synthesize spectrum with human occupancy using the baseline spectrum at the area of interest: (1) a SDR scans the spectrum from its lowest frequency to its highest frequency in an enclosed space with and without human occupancy, where labels are automatically assigned to the collected samples; (2) frequency bands sensitive to HOD are selected by the PCA algorithm; (3) a RF human signatures GAN (HSGAN) is proposed and trained with the average powers in the selected frequency bands of the baseline spectrum; (4) the trained HSGAN model synthesizes passive RF signals with human occupancy via the baseline spectrum without human occupancy collected in the enclosed space; (5) the trained HSGAN model predicts the human RF signatures in the enclosed space at a new location using the HSGAN model trained in other locations; (6) the HSGAN model is quantitatively evaluated via two classifiers including a CNN model and a KNN classifier for the quality of the synthesized spectrum; The experimental results show that the proposed HSGAN model is not only capable of predicting the human RF signatures using the baseline spectrum at the trained location but also it can produce human RF signatures using the baseline signals at a new location without training; in addition, a 99.5% correlation between synthesize human RF signatures and real human RF signatures results from the HSGAN.

1.3 Contributions

First, we explore feasibility of identifying the presence of one or more people inside an enclosed space by using passive RF signals via deep learning neural network, which to the best of our knowledge, is the initial research in this aspect. The main contributions of the initial research work are: (1) a new environment friendly and low cost approach to detect human occupancy in an enclosed space by collecting passive RF wireless signals from surrounding environment; (2) description of a system built during the experiment to implement our idea; (3) a CNN model to classify human occupancy that takes wireless RF raw data as input and produces detection results; (4) experimental results as an illustration of the feasibility of our proposed approach.

Second, the passive CR based CRhodora system provides following contributions: (1) adaptive spectrum sensing via reconfigurable CR is applied for HOD; (2) online training enhances system robustness for real-time performance; (3) results demonstrate traditional classifiers achieve better performance of human detection using much less training samples and number of frequency bands than the CNN.

Third, synthesis of passive human RF signatures via generative adversarial network contributes in below aspects: (1) a HSGAN model is proposed to synthesize passive RF data in the enclosed space and the proposed HSGAN model can generate human RF signatures via a baseline spectrum; (2) the trained HSGAN model can predict the human RF signatures in a new environment via transfer learning where the variation of wireless signals caused by human body are unseen during training; (3) the synthesized RF data is quantitatively evaluated by the HOD results and calculated correlation between the generated signals and real signals; (4) the comprehensive measured results are presented in this thesis for operational usability.

1.4 Thesis Outline

The rest of this thesis is organized as follows. Chapter Two introduces the related works. Chapter Three presents the initial research using software defined radio to passively collect RF data and applying CNN for HOD. Chapter Four details an advanced HOD system which dynamically reconfigures a CR to collect passive RF signals at different places of interest. Dynamic bands selection algorithms are applied to find the frequency bands sensitive to human occupancy when the baseline spectrum changes with locations. With the dynamically collected passive RF signals, four ML classifiers are applied to detect human occupancy. Chapter Five depicts the human RF signatures generation system via GAN to synthesize spectrum with human occupancy using the baseline spectrum at the area of interest; the HSGAN model and the quantitatively evaluated synthesis results are presented. Finally, Chapter Six concludes the thesis and points out future research directions.

CHAPTER TWO

RELATED WORKS

2.1 Human occupancy detection

Different technologies have been developed for HOD, or sometimes referred to as occupancy detection, including wireless detection and video surveillance. During the mid-90s, the subject of HOD began with infrared sensing [8]. Recently, passive wireless detection became popular as a wireless transceiver was not required to be carried by a human [10]. Li et al., used RFID tags in their experiment for human detection and behavior classification instead of passive RF [11]. Another systems depended on a Wi-Fi network to identify common occupant activities from Wi-Fi channel state information measurements [12]. Lv et al., made use of an active emitter to send wireless signals rather than using passive RF to quantify the quality of human actions via RF wireless signals [18]. Detecting objects for airspace surveillance by passive RF data was described in [13], but has not been applied to human detection in previous studies. Sparse vibration sensors estimated room-level building occupancy status by extracting human footsteps from the ambient vibrations [14]. This solution proposed by Pan et al. was restricted by the senor installation location to count entering and leaving room times. HOD inside vehicle was addressed by Birch et al., through color image segmentation techniques [15]. Shih et al. focused on human subject detection in a building by using a camera network [16]. Both solutions are not desirable when privacy is a concern. In order to compensate the solutions mentioned above, an occupancy detection solution is desired which should not depend on specific types of wireless signals nor introduce any concern of privacy. To make the system environment friendly and reduce the cost, the system should not emit active signals or occupy the limited communication channels. Furthermore, the deployment of the detection devices should be simple and adaptable.

2.2 Passive Sensing

Lidar, radar and ultrasonic sensors fall into the active sensing category, which includes a transmitter sending out a signal to be bounced back off the target and a receiver gathering the data upon its reflection. An example is micro-Doppler radar to discern humans from wildlife [17]. Opposite from active sensing, passive sensing techniques only detect or respond to certain type of input from the physical environment such as vibrations, light, radiation, heat or other phenomena occurring in the subject's environment. Passive sensing comes with the inherent advantage of not requiring an active signal source, and thus cannot be detected by observed parties as it only receives data. Compared to active modalities, implementing countermeasures against a passive modality becomes difficult, as rather than relying on a transmitter whose activity might be detected with equipment, passive modalities instead exploit information that can be collected without an active signal source. Several such examples of passive sensing-based technologies include photographic, thermal, electric field, chemical, infrared and seismic signatures. For example, an innovative photographic sensor was used to accurately control the defrosting process for a commercial size air source heat pump [18]. In the research [19], wildlife was detected by thermal cameras so that they could be protected from injuring and killing by the agriculture machinery. Mechanical seismic sensor system designed from paired geophones measures the field rotation rate [20]. A passive radar system based on Wi-Fi transmissions was investigated on two-dimensional target estimation problem [21]. Passively sensing RF signals has multiple benefits such as utilizing less the already crowded spectrum, avoiding third-party detection, and reducing power requirement. Passive wireless signals are available almost anywhere except extreme environments such as under the sea. Our HOD system over passive RF analysis system does not depend on any specific wireless signal types such as Wi-Fi or cell network.

2.3 Deep learning

Deep learning has shown its effectiveness in many fields such as automatic speech recognition, image recognition, visual art processing, natural language processing, customer relationship management, recommendation systems, financial fraud detection, etc. Recently, some researchers have initialized the study of radio signal modulation recognition and wireless interference identification by using convolutional neural network (CNN) through the collected passive RF data. In [22], experiment was conducted to classify different modulation formats. Paper [23] presented the research work of deep learning-based radio signal classification by comparing CNN and residual neural network (RNN). However, the studies in [22] and [23] primarily focused on the characteristics of wireless signals themselves instead of their applications. Authors of [24] introduced an approach to detect and identify a specific radio transmitter uniquely among other similar devices by using software defined radio (SDR) and CNN. Researchers of [25] have also conducted an experiment to classify the emitter of the wireless signal. Article [26] depicted the experiments of using CNN and deep neural network (DNN) to identify rogue RF transmitters. But [24]–[26] focused on the scope of the wireless system. The study conducted in [13] showed a CNN system being used to assess the quality of human actions via RF wireless signals. However, the research in [13] used an active emitter to send wireless signals rather than using passive RF.

Human presence detection is addressed by research work in [11] where RFID tags were used in the experiment for human detection and behavior classification instead of passive RF. The research of [27], [28] are focused on the analysis of human activities by using deep learning to process wireless RF signals. However, active radio signals were still used in these experiments. Passive RF data was utilized to detect objects in paper [29] but deep learning was not used in this study. By utilizing a deep learning neural network for wireless signals classification, the network can potentially achieve better performance in a complex wireless signal environment. None of the studies mentioned above and papers mentioned in [30] used wireless passive RF signals to classify the human occupancy inside an enclosed space through a deep learning neural network. Based on the existing research, the feasibility of using deep learning to analyze passive RF data to detect human occupancy in an area of concern, is addressed in this research.

2.4 Cognitive radio

A software defined radio (SDR) is a radio communication system which utilizes a group of technologies including hardware and software. Some or all functions of the radio are reconfigurable through software or firmware which are operated on the programmable processors. SDR has many applications in various fields such as spectrum monitoring [24], RF transmitter identification [25] and other areas. For example, it was used as a receiver to estimate mobile station's location through received signal strength [31]. Bonoir et al. applied SDR to remote wireless tomography in their experiment [32]. In the research work, SDR was used to recognize gesture through Wi-Fi signals by Zhang et al. [33]. CR has evolved from SDR by adding additional functions including sensing its environment, tracking changes, and reacting upon its findings by reconfiguring its setting. As described by Jondral, CR emerged in recent decades due to the rapid deployment of new wireless devices and applications [34]. The inefficient usage of limited spectrum resources by the fixed channel allocation policy urges this innovative technology to be applied quickly and widely. CR enables the development of dynamic spectrum access network which can utilize the spectrum and energy more efficiently in an opportunistic fashion and void the inference with licensed users [35]. A general metric is proposed by Wang et al. to facilitate the configurable balanced trade-off between spectral efficiency and energy efficiency for CR [36]. Liu et al. proposed a cluster-based cognitive industrial internet of things to improve the spectrum sensing and the performance of transmission through CR [37]. Power consumption can be saved by actively predicting the channel utilization status through sensing the spectrum with CR device versus continually scanning the wireless environments [38], [39]. Furthermore, reinforcement learning is applied by Lin et al. to power allocation of the transmission channel and the control channel in CR network reduces the wasting of power [40]. Energy can be saved by incorporating the CR communication network with the smart grid which automatically monitors and controls grid activities [41]. Joshi et al. surveys CR wireless sensor networks and its potential application areas to military and security, health care, home appliances, real-time surveillance, transportation and vehicular networks and so on [42]. The encouraging results of these existing applications indicates that CR can be an ideal candidate for HOD via passive RF sensing.

2.5 Feature selection

There are three common elements that classification is based on, signals, features, and decisions. Processing all the signals is expensive, while decisions lack completeness, so most approaches seek feature analysis. In ML, feature selection is the process to automatically or manually determine features for decision making. Feature selection can remove the redundant or irrelevant features in the data without losing much of information. Feature selection can simplify the model, shorten the training time, and further enhance model generalization. The confidence (or credibility) of classification can be improved by dynamically determining how many features are necessary and which features are salient. The feature selection process falls into three categories, supervised, semi-supervised or unsupervised depending on the availability of labels of the data, fully available, partially available or none, respectively. Dynamic feature selection is a widely popular technique to demonstrate efficient and adaptive solutions using clustering algorithms applied on RF data. Recent books highlight the advantages of ML and deep learning to RF imagery and communications data [43]. In the real time system, radio modulations were properly classified by only selecting a small portion of spectral correlation density that can be used to classify signals without the need for system synchronization [44]. Feature selection was identified as the core step by Wang et al. to secure wireless transmission via RF distinct native attribute [45]. The indoor location estimation was optimized by adding the feature selection phase to the methodology which was performed through genetic algorithm (GA) [46]. All the research works mentioned above indicate that ML can benefit from feature selection technique.

2.6 Generative Adversarial Networks

The wireless environment is difficult to control and is vulnerable to jamming signal disturbance sent by malicious devices. Knowing and inspecting the spectrum at the location of interest becomes an indispensable part of HOD from wireless signals. Researchers have initiated various approaches to protect the security of wireless environment. SDR and CNN were used by Riyaz et al. to detect and identify a specific radio transmitter uniquely among other similar devices [24]. The emitter of the wireless signal was classified by four ML algorithms from the adversarial devices by [25], [47]. However, both research works mention passively monitor the wireless environment instead of proactively predicting spectrum variations. Generative models in ML project the changes in the wireless network. The GAN was proposed by J. Goodfellow et al. in 2014 to estimate the generative model via the adversarial process [48]. The GAN has been widely employed in multiple areas and drew attention from some researchers in the field of wireless communication due to its capability of synthesizing data. Roy et al. [26] used the RF data generated by GAN to simulate the spoofing signals thus the rogue transmitters could be recognized from the trusted devices through the classifier which was trained with the simulation data and trusted data. Missing spectral information was recovered via GAN by Tran et al. [49] in domain of a ultra-wideband (UWB) radar system. Li et al. [50] implemented sparsely self-supervised GAN to estimate the corrupted cellular network data. The significant accuracy improvement was made by Liu et al. [51] in the field of real-time smartphone indoor localization via GAN. With these very promising outcomes from the above studies, there is motivation to apply GANs to train a generative model which can predict human RF signatures through the baseline spectrum via the adversarial process.

CHAPTER THREE

OCCUPANCY DETECTION VIA DEEP LEARNING

3.1 Introduction

This research is conducted under assumption that human subjects will produce signatures in the collected passive RF signals of the corresponding location. The presence of human subjects, the size and the speed of the subjects will alter the RF signals, and the subtle variation can be detected by the neural network.

3.2 Advantages

The usage of passive RF data shares some of the same traits with passive radar systems in which no actively transmitted signals are required, and the object is detected through third party emitters. In addition to that, both passive radar and the proposed solution have low power consumption and are difficult to detect. Both solutions can be used to find a moving target and monitor an air space when the target is not visually observable. Because the solutions do not use an active emitter and only collect passive RF signals from the surrounding environment, the solution does not introduce radio spectrum pollution into the increasingly crowded wireless space. This approach does not generate any interference with the existing wireless system due to only collecting passive RF data. A desirable trait as wireless signals transmission is restricted in certain areas. Due to the nature of the modality, the system possesses a larger detection coverage and is not as limited by factors such as installation angle and position, unlike other methods. Because the solution is reliant on passive RF, the installation costs and complexity are greatly reduced. Ambient RF signals exist everywhere, which can be utilized for human subject detection. Therefore, this approach is not limited by location. Nor is it limited by factors such as light or weather conditions either. Further investigation of the impact of extreme weather conditions such as thunder and lightning to the system is still required. In addition, the solution also costs less without active emitter present.

3.3 Technical Approach

In this experiment, the presence of one or more people in an enclosed space such as an office room or a home study room is addressed. At the time when this experiment was conducted, there was not traditional signal processing algorithms were applied for processing such complex patterns; no existing formula or algorithm has been attested to solve this problem; there is no evidence to prove this is a linear problem. Deep learning is noted for having excellent pattern recognition capabilities and excellent performance for solving nonlinear problems with unknown relationships. Motivated by recent advances and the remarkable success of CNN, the initial study focuses on applying CNN to solve this problem. Shared weights and biases greatly reduce the number of parameters involved in a CNN. The convolutional layer will reduce the number of parameters it needs to get the same performance as the fully connected model. It will result in faster training for the convolutional model, and ultimately help to build deeper networks. The pooling layers simplify the information in the output from the convolutional layer. In detail, a pooling layer takes each feature map output from the convolutional layer and prepares a condensed feature map. With the computation capability of CNN, it can be trained with enormous data by consuming less time comparing to the fully connected deep neural network [24].

In order to teach CNN model to detect human occupancy, adequate training data needs to be collected. SDR is adopted by our research to collect passive RF signals. SDR is a radio communication system where components that have been implemented in hardware are implemented by software on a personal computer or embedded system. SDR defines a collection of hardware and software technologies where some or all the radio's operating functions are implemented through modifiable software or firmware operating on programmable processing technologies. There are several benefits of using SDR to collect the RF raw data, such as being easy to process with software programs, having a wide range of utility, and providing a cost-effective means of implementing software upgrades.

3.4 Experiment Design

Passive RF signal HOD system is developed during our experiment and is described in Figure 1. It is composed of three subsystems: data acquisition, data preprocessing, and classification. The antenna collects the passive RF signals in an enclosed space sent by opportunistic transmitters. These signals are in turn preprocessed by SDR and then converted from analog signals to digital raw stream data. From there, the raw stream data is then preprocessed before it is fed into CNN model. Finally, the person presence probability is calculated by CNN model and the classification result is sent through its output layer. The details of the experiment are given in the following subsections, including RF signal acquisition, RF signal pre-processing, experimental scenarios design, CNN model training and HOD.

3.4.1 RF signal acquisition

To eliminate the contamination of the data from irrelevant electronic devices, only

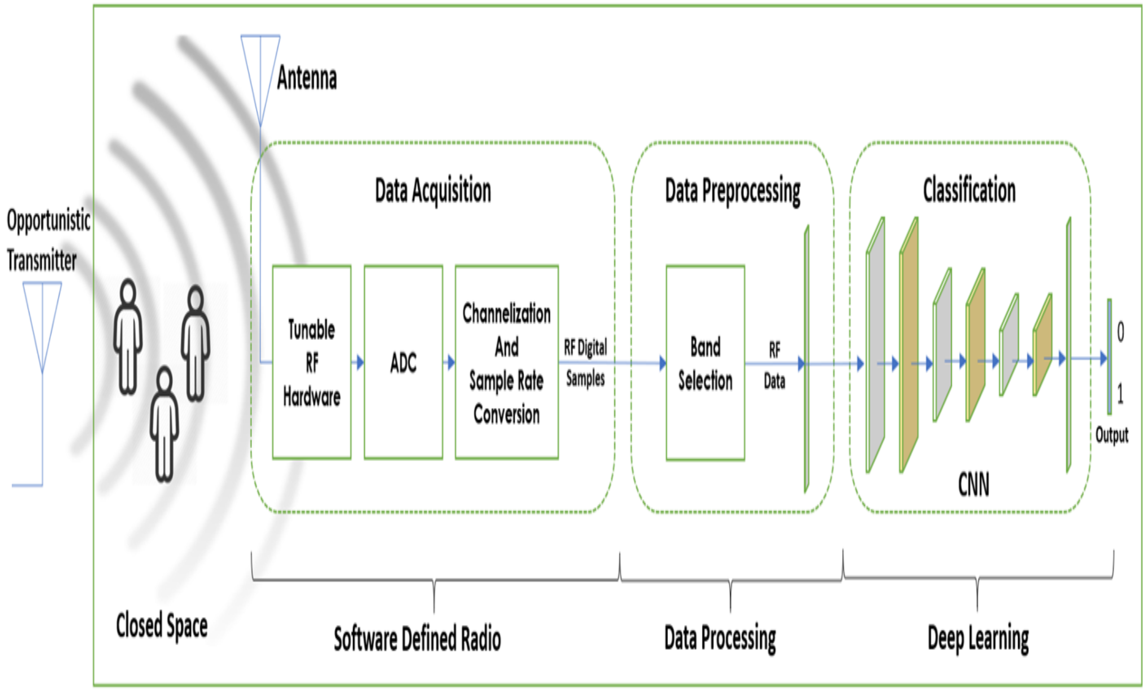

Figure 1. Human occupancy detection system.

the laptop and SDR used to collect data and a personal cell are powered on in the enclosed space during data collection. The laptop and SDR always work regardless the occupancy status. To simulate the real-life environment that people carry the cell phone in most situations and make sure our system does not depend on the signals emitted by the cell phone, the cell phone is left power on or off in the enclosed space randomly regardless the occupancy status. Passive RF raw data collection is described in Table 1. RTL2832U is used to collect RF raw data at two separate locations, a study room in a single-family house and a fourth-floor office in a six-floors building, with and without human occupancy. Labels are assigned to RF raw data automatically during data collection.

The SDR continuously scans the spectrum from the lowest frequency 2.4 MHz to the highest frequency 1760MHz. The sample rate of 2.4 MHz is chosen in our experiment because it is the verified highest sample rate at which the regular universal serial bus (USB) controllers do not lose samples although the theoretically possible sample rate is 3.2 MHz. RF raw data is collected, with and without known primary signals such as FM, TV, and cellular passive signals, at the locations of interest. Selective frequency band and full frequency band RF raw data is collected.

A total number of 197 selective bands are chosen by adaptive step, meaning that small scan steps are used for active bands and large scan steps are used for inactive bands. Step size is set based on FCC Table of Frequency Allocations, observation of frequency spectrum at collecting location through SDR and local radio station frequency list.

Full band includes all frequency bands with an even step size of 1.2MHz. 4800 samples per frequency band are collected at sample rate of 2.4MHz during each 2 milliseconds. 2 milliseconds per frequency band is adopted so that sufficient number of signals can be collected to maintain the detection accuracy and the system can be fast enough to monitor the occupancy status in real time. At each experiment location, the study room and the office, the antenna is placed at a fixed position and direction is fixed. Two identical SDRs are used to collect the data which can reduce the data collection time and can eliminate the device dependency. Both selective bands and full band is scanned with the same setting of sample rate, duration and period as listed in Table 1.

Table 1. Passive radio frequency data collection.

Items	Description
Collection Device	RTL2832U
Location	Closed space: an office and a home study room
Human Presence	0: No person in an enclosed space; 1: One or more person in an enclosed space
Data Labelling	Automatically assign scenario ID (0 or 1) and location ID to collected RF raw data
Frequency Range	From 24MHz to 1760MHz
Frequency Band	Selective Band: small step for active bands, large step for inactive bands
Selection	Full band: even step 1.2 MHZ
Sample Rate	2.4MHz
Period	Continually collecting for a few hours each time
Duration	2 milliseconds per frequency band

3.4.2 RF signal pre-processing

The RF raw data collected at the 197 selective bands is fed to neural network directly with required format and no further frequency band data extraction is needed. Data preprocessing is then applied on full band RF raw data to extract band data of interest. These extraction bands are: active bands including and excluding cell network bands, inactive frequency bands including and excluding cell network bands, and random frequency bands. The number of each frequency band is listed in Table 2.

The extraction method is described as below. In order to determine what bands are active and inactive, a continuous 48 hours full band RF raw data is collected at home

Table 2. Frequency band selection.

Frequency Band Group	Number of Band
Selective Band	197
Active Band	76
Active Band Excluding Cell Network Band	53
Inactive Band	137
Inactive Band Excluding Cell Network Band	94
Random Band	128

study room and this data is used to calculate average power in the spectrum. To estimate the power spectrum, the average power per frequency band is calculated. The number of samples per frequency band, denoted by N, is 4800. $p(f)$ is the average power of frequency band centered at f and is calculated as below,

$$p(f) = 10 * \frac{log_{10}\left(\sum_{i=1}^{N} a_i(f)^2\right)}{\frac{N}{2}} \tag{2.1}$$

where $a_i(f)$ is the amplitude of the i-th intermediate frequency signal received by SDR at the frequency band of f. Let M be the number of full band samples which are collected within these 48 hours. $p_{avg}(f)$ is the average power spectrum estimated over M full band samples calculated by $p_{avg}(f) = \sum_{j=1}^{M} p_j(f)/M$, where j is the index of the power

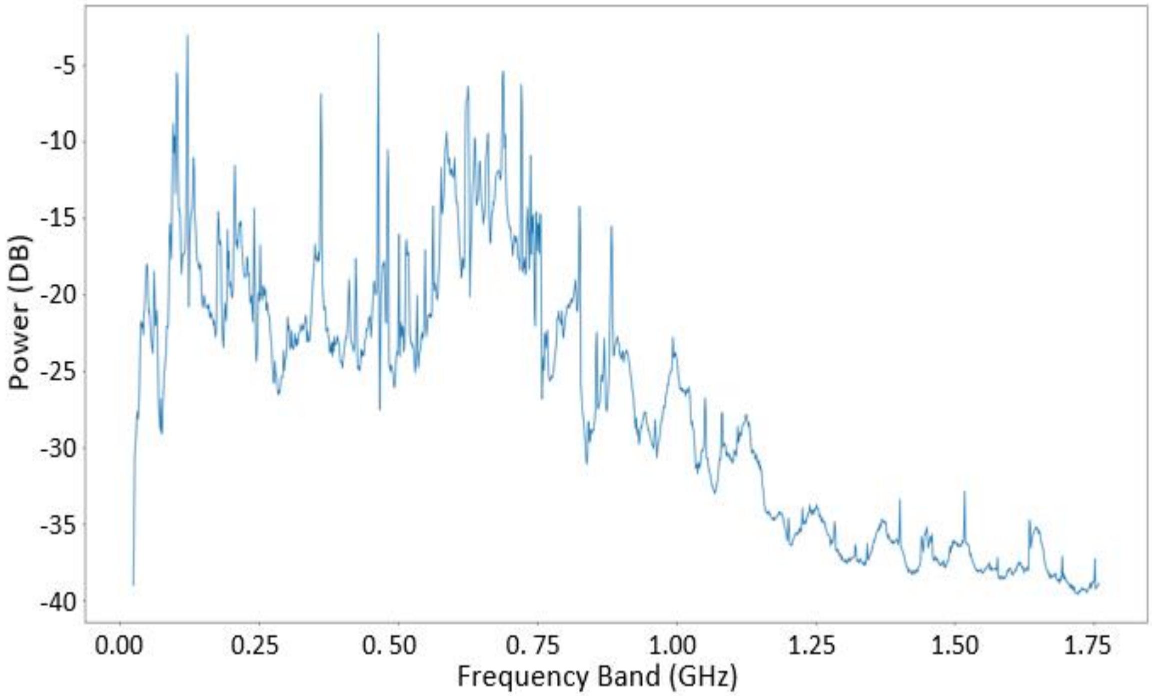

Figure 2. Average frequency band power in the spectrum.

spectrum samples. The average frequency band power in the spectrum ranges from 24MHz to 1760MHz, within these 48 hours as shown in Figure 2.

Frequency bands with peak average power in the spectrum are selected as active bands. Frequency bands with valley average power in the spectrum are selected as inactive bands. AMPD algorithm [17] is then used to automatically detect the peaks and valleys in the spectrum. Active and inactive bands are selected according to the detection results. Cell network bands are then excluded from the active bands and inactive bands to form active bands excluding cell network bands and inactive bands excluding cell network bands. Random bands consist of 128 randomly selected bands from full band.

Table 3. Experimental scenario design

Name	Bands	Location	Time
ActH	Active Band	Home	-
ActHNCell	Active Band Excluding Cell Network Band	Home	-
InH	Inactive Band	Home	
InHNCell	Inactive Band Excluding Cell Network Band	Home	-
RndH	Random Band	Home	-
RndO	Random Band	Office	-
SelHO	Selective Band	Home & Office	-
SelH	Selective Band	Home	-
SelO	Selective Band	Office	-
ActHT1	Active Band	Home	6AM to 12PM
ActHT2	Active Band	Home	12PM to 6PM
ActHT3	Active Band	Home	6PM to 12AM

3.4.3 Experimental scenarios design

A total number of 12 experimental scenarios are designed and listed in Table 3. These scenarios cover HOD, accuracy and sensitivity tests against band selection, location diversity, and time difference. The scenarios are then categorized into 3 groups as listed in Table 4, band, location and time. These band sensitivity tests consist of 6 scenarios listed under the Band category. ActH is designed to train and test the CNN model with 76 active frequency bands RF raw data collected at home. Scenario ActHNCell is designed to train and tests the CNN model with 53 active frequency band

Table 4. Number of bands used in different scenarios.

Category	Experimental Scenarios	# of Band
Band	ActH	76
Band	ActHNCell	53
Band	InH	137
Band	InHNCell	94
Band	RndH	128
Band	RndO	128
Location	SelHO	197
Location	SelH	197
Location	SelO	197
Time	ActHT1	76
Time	ActHT2	76
Time	ActHT3	76

excluding cell network band data collected at home. Scenario InH is designed to train and test CNN model with 137 inactive frequency bands RF raw data collected at home. Scenario InHNCell is designed to train and test CNN model with 94 inactive frequency bands data excluding cell network bands data collected at home. Scenario RndH uses randomly selected 128 band RF raw data collected at home to train and test CNN model. Scenario RndO uses the same 128 frequency band to extract RF raw data collected at

Table 5. Convolutional neural network dataset.

Scenarios	# of Training Samples	# of Validation Samples	# of Test Samples
ActH	2400	600	170
ActHNCell	2400	600	170
InH	2400	600	170
InHNCell	2400	600	170
RndH	2400	600	170
RndO	1200	300	92
SelHO	12480	3120	820
SelH	4560	1140	300
SelO	7920	1980	520
ActHT1	2512	327	86
ActHT2	2512	327	86
ActHT3	2512	327	86

office. Location sensitivity test consists 3 scenarios listed under Location category. The 197 selected bands RF raw data collected at home and office are used to train and test CNN model. SelHO consists raw data of home and office, SelH only uses data of home and SelO only uses data of office. Time sensitivity test consists 3 scenarios listed under Time category. 76 active band RF raw data collected at home is used to train CNN Model. ActHT1 uses RF raw collected from 6am to 12pm to test CNN model, ActHT2 uses data from 12pm to 6pm for testing and ActHT3 uses data from 6pm to 12am for testing.

3.4.4 Training Data

The RF raw data is split into training dataset, validation dataset, and test dataset. The number of training, validation and test samples of each scenario is listed below in Table 5.

3.4.5 CNN Architecture and training

The CNN consists of one 2D input layer, four 2D convolutional layers, one flatten layer, one fully connected layer and one output layer. The same CNN structure is used across all experimental scenarios except for the input layer row number. The input matrix consists K rows, which corresponds to frequency band number listed on Table 2, and 4800 columns, which is the sample number per frequency per one collection duration. The value of input matrix is RF raw data collected by SDR.

1D vector kernel is used to extract features from the frequency band raw data. The same 1D kernel shape $[1 \quad 4 \quad 8 \quad 8]$ is then used across these four convolutional layers along with the same stride step $[1 \quad 1 \quad 1 \quad 1]$. ReLU activation function $f(x) = \max(0, x)$ is used across all these four convolutional layer and fully connected layer. After the convolutional layers is the flatten layer. Connected to the flatten layer is the fully connected layer. The output layer has two perceptron which represents the human occupancy status. The values of the two binary numbers, indicate if human occupancy is detected or not. Other CNN architectures have been designed, trained and tested as well. But they did not achieve better performance than the one described above.

The CNN model is trained and evaluated for each experimental scenario listed in Table 3. The trained CNN model is used to process RF raw test data and detects the human occupancy in the enclosed space.

3.5 Experiment Results

The expected overall experiment result of the initial phase is that CNN can distinguish human occupancy in an enclosed space by collected passive RF signals. In order to determine if this is the case, an F1 Score needs to be calculated in order to quantify the overall accuracy of the neural network, measuring the precision and recall of the results. The actual performance is evaluated by a confusion matrix with the equations below.

$$accuracy = \frac{TF+TN}{TP+FN+TN+FP} \tag{3.1}$$

$$precision = \frac{TP}{TP+FP} \tag{3.2}$$

$$recall = \frac{TP}{TP+FN} \tag{3.3}$$

$$F1 = \frac{2 \times precision \times recall}{precision+recall} \tag{3.4}$$

The overall experimental accuracy is shown in Figure 3. Both accuracy and F1 score from 10 experiments out of 12 is more than 90%. The accuracy and F1 score corresponding to the scenarios of ActH, ActHNCell, SelO and ActHT1 are higher than 95%. The band sensitivity test results are shown in Figure 4. The experiments compare scenarios without cell network band data vs with cell network band data. Both scenarios achieve relatively close performances. For example, both accuracy and F1 score differences between ActH and ActHNCell is 1.2%. However further research is required to determine why the inactive band scenarios InH and InHNCell achieve similar performance as the active band scenarios ActH and ActHNCell.

The location sensitivity test result is shown in Figure 5. It can be seen the performance of SelH is slightly lower than the other two scenarios. The performance difference among locational test scenarios is less than 6%, which means the system is not very sensitive to location difference. The time sensitivity test result is shown in Figure 6. The performance is the best in the 6am to 12pm time period and the worst in the 6pm to 12am time period. The cause of the difference is not clear at the moment. It might be due to the small test sample size or the variation of noise level with time. Further investigation is needed to improve the robustness over time.

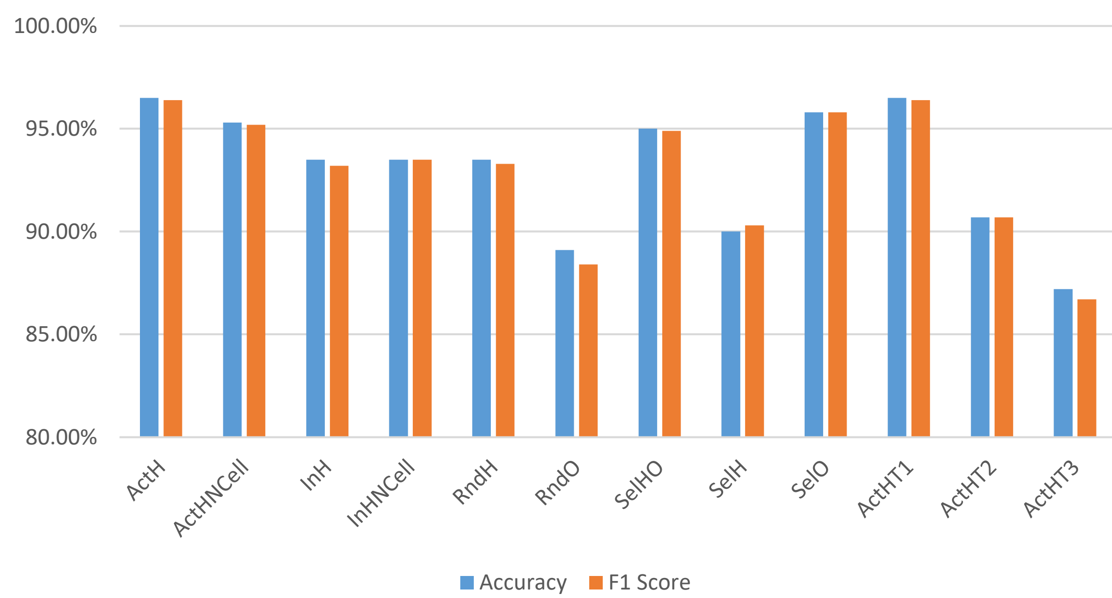

Figure 3. Overall accuracy.

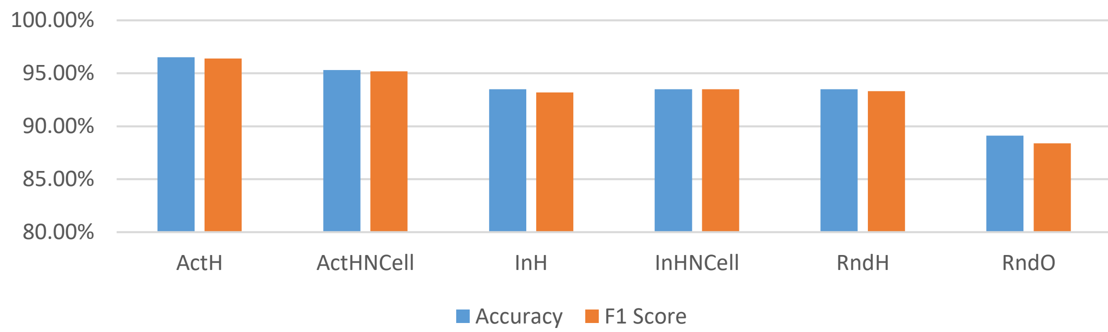

Figure 4. Band sensitivity.

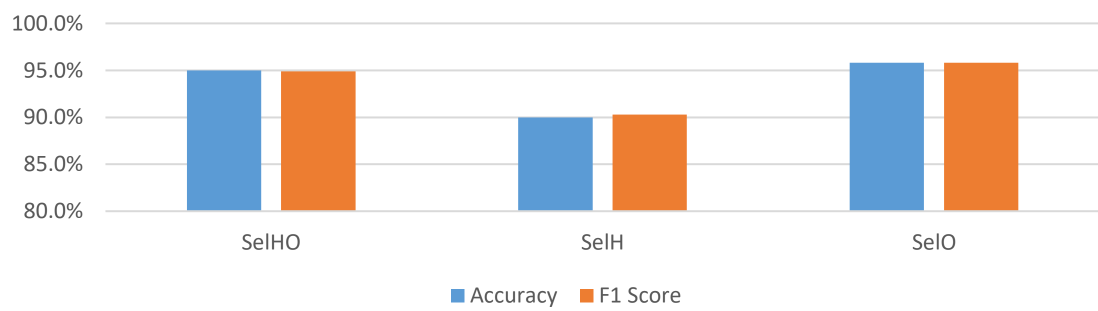

Figure 5. Location sensitivity.

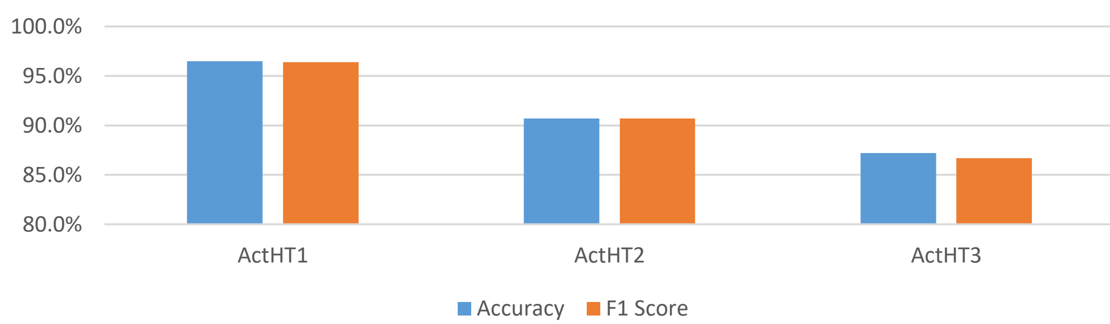

Figure 6. Time sensitivity.

3.6 Summary

The results of this experiment indicate that human occupancy can be detected by passive RF wireless signals via deep learning neural network in an enclosed space. Robustness is verified by testing against different frequency bands, locations and time periods. However, this system can only work in a fixed location and must use the spectrum of a large number of frequency bands. To make the system more robust and efficient, further research is conducted in phase two.

CHAPTER FOUR

OCCUPANCY DETECTION VIA COGNITIVE RADIO

4.1 Introduction

Human occupancy in an enclosed space was successfully detected via deep learning of passive RF data in phase one. The initial experimental results indicated that the variation of the baseline environment spectrum caused by human occupancy can be detected by CNN. To the best of our knowledge, it was unknown how human occupancy changes the spectrum sensed by CR before our study. To attack this problem, ML is utilized in the second phase. ML has been widely used on RF data analysis due to it intrinsic capability of learning. ML can automatically learn the pattern by observing the labeled RF data and obtain the desired knowledge. The well-trained ML model can make good decision to detect occupancy based on the RF samples provided and it has been examined in phase one.

The frequency band in a normal environment is widely distributed from 500KHz to 8.4GHz. It is not economic or feasible to use full band data for HOD. Passive wireless signals cannot be controlled as the spectrum changes over the time and is different from location to location. Per spectrum observation recorded with and without human occupancy, certain frequency bands are sensitive for human detection. These sensitive frequency bands should be identified in different environments and automatically determined to eliminate human effort. CR is an adaptive intelligent radio technology which enables the radio to automatically sense the surrounding wireless spectrum and reconfigure its parameters to improve its operating behaviors. CR is the ideal candidate to accomplish dynamical frequency band selection per its reconfigurable characteristic and to proactively adapt to different environments.

Due to the constantly changing wireless environment, a feedback loop control mechanism is needed to maintain optimal detection performance. To design the control loop, an online training approach is depicted as the following. A trained ML model which can detect human occupancy in an environment is established as the base model. Online training is applied on this base model by retraining it with newly collected and dynamic selected RF band data at a regular basis depending on the fluctuate level and changing frequency of the wireless signals. The model is updated over time to maintain its detection accuracy.

4.2 Advantages

Feature selection algorithms are applied to dynamically select frequency bands which are sensitive to HOD and reconfigure the CR without scanning the whole spectrum in its working range. Only the selected frequency bands data is used to train ML classifiers for HOD. There are several advantages offered by this dynamic bands selection strategy: (1) a reconfigurable CR significantly reduces power consumption; (2) the system can maintain a robust performance in different locations and time by adaptive spectrum sensing; (3) the system shortens the time needed for system deployment as the

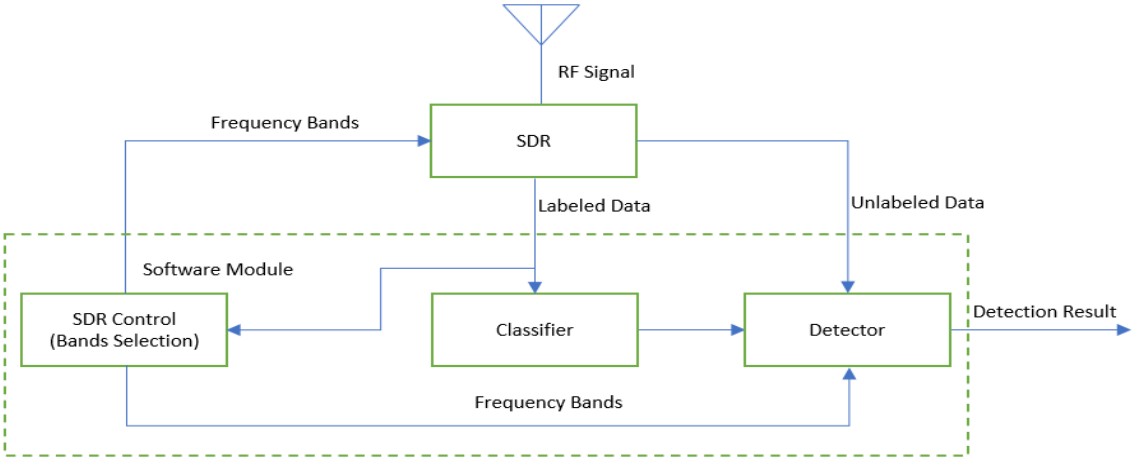

Figure 7. Cognitive radio based occupancy detection system.

bands are selected automatically without human interaction; (4) it is data efficient and interpretable using classic ML models instead of deep learning neural network.

4.3 Technical Approach

The improved the efficiency of the HOD system and reduce the data needed to train the ML model, CRhodora is developed in this phase. The proposed CRhodora system includes a receiving antenna, an SDR, and a software module that detects human subject and reconfigures SDR for optimal performance. The system diagram is depicted in Figure 7. The RF signals are collected from enclosed spaces. In the initial stage, the SDR is configured by SDR control to scan the whole spectrum in its frequency range and the collected data is labeled. The labels associate the collected RF signal with the corresponding human occupancy status. Frequency bands which are sensitive to human occupancy are selected after enough samples of the whole spectrum are collected. The SDR is reconfigured by the SDR control module to scan the selected frequency bands only. Next, the classifier is trained with the selected frequency bands samples to detect human occupancy. The detector uses the trained classifier and the passive RF signals to continuously monitor human occupancy. The frequency bands selection and classifier are updated periodically in a user specified time interval so that the system can adapt to the spectrum varying with time and locations. Finally, the detector is updated with the adaptively trained classifier and uses the selected frequency bands for detection. Rhodora approach is explained further in the following subsections as RF signal acquisition, RF signal pre-processing, adaptive spectrum sensing and classifier training.

4.3.1 RF signal acquisition

The data collection is similar to the data collection in phase one described in Table 1 except following two changes: (1) RF raw data is collected at three separate locations including a study room in a single family house, a bedroom in an apartment and a car parked in open space; (2) only full band is scanned and the spectrum is continuously scanned by the SDR with even step size of 1.2MHz from the lowest frequency 24MHz to the highest frequency 1760MHz. The data collected through a full band scan is referred as a full band sample. One full band sample contains the raw data of 1447 frequency bands.

At each experiment location, the antenna is placed at a fixed position with fixed directions. A human subject can occupy different positions in the enclose space. Figure 8 illustrates the data collection environments and antenna setup. The antenna is placed at the corner of the study room and the bedroom, and at the front passenger seat in the car.

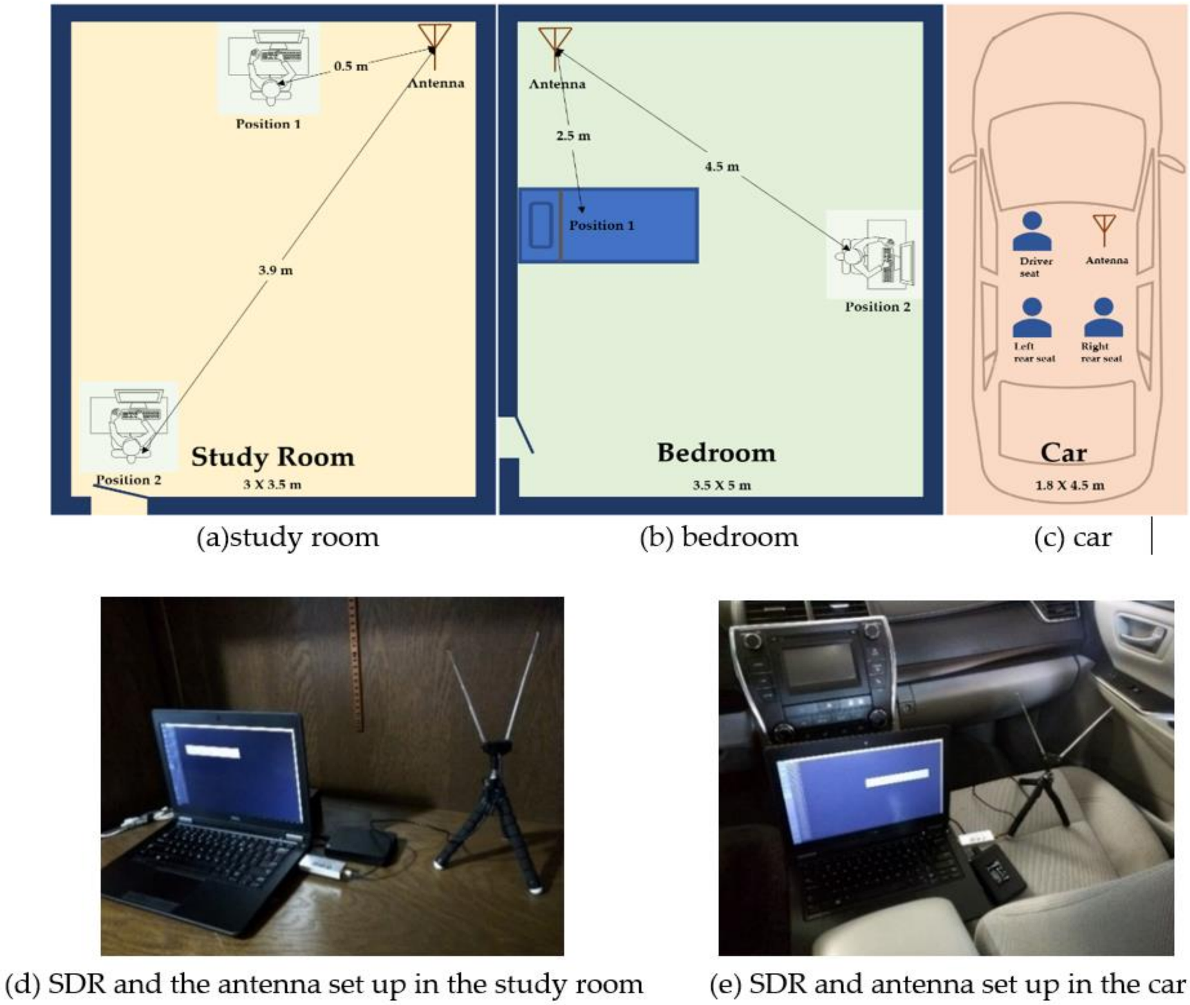

Figure 8. Data collection setup.

A human subject stays at a position without walking and other significant motions during data collection. In the study room, the distance between Position 1 and the antenna is around 0.5 meter and the distance between Position 2 and the antenna is 3.9 meters. For distances in other experiments, please refer to Figure. 150 full band samples are collected without human subjects at each location and total 450 full band samples are collected at these three different locations. 150 full band samples are collected when a human subject presents at a position in that enclose space and without other human subject present at the same time at that location. The same data collection is performed for each position of each location. 300 full band samples are collected in the study room, 300 full band samples are collected in the bedroom and 450 full band samples are collected in the car with human presents. To eliminate the impact of spectrum variation among different timeframes in the day, the RF data collection with and without a human subject occupying the space is performed in the similar time period of the day at each location. For example, the data collection in the car only conducted in the afternoon time from 1 PM to 6 PM. It takes a few days to collect data for each location. Two identical SDRs are used to collect data to reduce data collection time and eliminate the device dependency.

In order to verify how well the system works at different locations and different environments, experiments were carried out at several locations. They are Position1 in the study room (StRmP1), Position2 in the study room (StRmP2), Postion1 in the bedroom (BdRmP1), Position2 in the bedroom (BdRmP2), Driver seat in the car (CrP1), Left rear seat in the car(CrP2), and Right rear seat in the car (CrP3). The system detects human occupancy but does not estimate the subject’s location or the exact number of human subjects.

4.3.2 RF signal pre-processing

To estimate the power spectrum, the average power per frequency band is calculated. $p(f)$ is the average power of frequency band centered at f and is calculated using the same equation (2.1). Let M be the number of full band samples, which is 150 in our

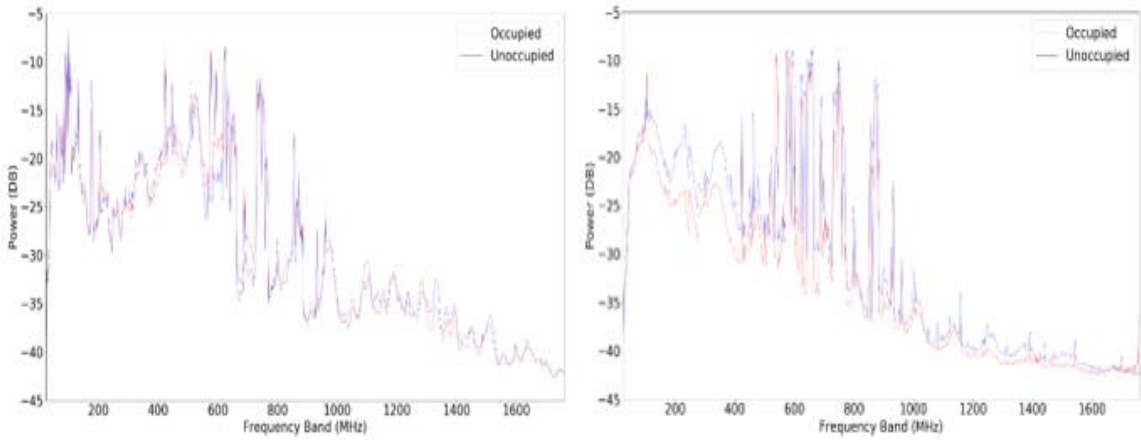

(a) Study room, position 1 occupancy (b) Car, driver seat occupancy

Figure 9. Average power spectrum.

experiment. $p_{avg}(f)$ is the average power spectrum estimated over M full band samples calculated by $p_{avg}(f) = \sum_{j=1}^{M} p_j(f)\,/M$, where j is the index of the power spectrum samples.

Snapshots of the power spectrum at different locations are shown in Figure 9. The red line is for occupied situation, while the blue line is for unoccupied situation. There are noticeable differences between the spectrums of occupied and unoccupied scenarios at each location. The degree of variation between the two scenarios is location dependent. For example, the spectrum variation is larger inside the car than that of study room. The results are probably affected by factors such as body mass of the human subject, the materials inside of the enclose space, the spectrum or other unknown factors. For example, the metal material in the car may cause the large variation. The cause and the environmental variation shall be further investigated in the future research.

4.3.3 Adaptive spectrum sensing

The power spectrum measured by SDR varies with time and location. The devices which transmit signals can be added or removed and it is difficult to predict the precise transmission usages. For example, more wireless channels are used during daytime when there are more human activities, while less signals are transmitted during the night. Many radio stations only transmit at certain hours every day. The spectrum also varies by location as the RF signals tend to be sparser in rural areas than in crowded cities. The Wi-Fi is stronger in places where more people tend to visit more frequently. Even in the same location, the environment setup such as building materials, furniture in a room, the electronic devices used and so on can add further variation to the spectrum. The spectrum sensing must be adaptive to these changes to guarantee robust performance. On the other hand, it is inefficient to use the whole power spectrum for occupancy detection. The prolonged scanning time per cycle leads to lower time resolution and waste power. For these two reasons, adaptive spectrum sensing is desired to improve the robustness and efficiency of the system.

Opportunistic spectrum access through reconfigurable CR has been well studied by many researchers [52]–[54] to adapt the constantly changing wireless environment in the real time manner, improve system performance and reduce the power consumption. In our study, adaptive sensing is realized by dynamically selecting the frequency bands that are sensitive to HOD at various locations and time. The baseline power spectrum is adjusted accordingly.

It is well known that good feature selection can help improve classification performance [55]–[57] The frequency band selection process aims to remove the bands that are not sensitive to human occupancy and only keep those sensitive ones. Average power of each frequency band $p_{avg}(f)$ is calculated during data pre-processing. Our observation of the measured power spectrum finds that the power of many frequency bands does not have noticeable change between the occupied and unoccupied scenarios. This suggests that optimal frequency band selection can result in significant dimension reduction of data. An automatic process is desired to for dynamic frequency band selection. Supervised feature selection requires labeled data while unsupervised feature selection can work with unlabeled data. For evaluation purposes, a PCA based unsupervised selection algorithm and an RFE-LR supervised selection algorithm are implemented to compare their frequency band selection results.

4.3.3.1 PCA based frequency band selection

Classic PCA is an algorithm which can reduce dimensionality of a dataset and increase the interpretability of data while minimizing information loss. It has been widely applied in data analysis, data processing and dimensionality reduction. However, classical PCA methods are not associated with a probability density and cannot be extended to a mixture of probabilistic models, which is usually the case of unsupervised learning and feature selection. To overcome this limit, a number of approaches have been attempted to formulate mixture models. Most of these approaches are two-stage procedures with the first step partitioning the data space followed by estimation of the principal subspace within each partition, i.e. local PCA. Tipping and Bishop proposed a probabilistic PCA (PPCA) model, which can be naturally extended to a mixture of local PCA models [58]. The PPCA method estimates the probabilistic model by the maximization of a pseudo-likelihood function and avoids an explicit two-stage algorithm.

In this research, we apply the PPCA algorithm with $p(f)$ as the input features to extract principal components from the power spectrums of different locations.

As each principal component is a linear combination of all the original frequency bands, if the system directly uses the extracted principal components as features, the interpretation of the results and subsequent spectrum sensing still has to involve all of the bands even if only a few components are kept. So we select frequency bands according to their loadings in the extracted components [59]. Once principal components are extracted, they are ranked from high to low by importance according to the variance they can explain, and the first three components are kept. Finally, k ($k \in [10, 150]$) frequency bands with the highest absolute coefficients in the first three components are selected.

4.3.3.2 RFE-LR based frequency band selection

RFE recursively removes the weakest feature and considers smaller and smaller sets of features until the specified number of features is reached by fitting an estimator which assigns weights to features. RFE is computationally less complex using the feature weight coefficients or feature importance comparing to sequential backward selection (SBS) which eliminates features based on user-defined classifier or regression performance metric. RFE was applied to select features used to measure the transient stability in the power system [60]. Most significant features were chosen by SBS to analyze the auditory evoked potential parameters in the presence of radiofrequency fields [61]. RFE is applied in our study to reduce the computation cost in the real time system. Logistic regression (LR) with L2 regularization and the variation of limited-memory Broyden Fletcher Goldfarb Shanno (L-BFGS) optimization [62] is chosen as the estimator when applies RFE in our research. Initially, the values of $p(f)$ of these 1447 frequency bands and corresponding 1477 labels which values are 1 or 0 are fed to LR estimator. The coefficients are obtained by training LR estimator. A certain number of frequency bands with the smallest coefficients are removed and the rest are kept. Then the first round of least significant frequency bands elimination finishes. The $p(f)$ of remaining frequency bands and corresponding labels are used in the next round feature elimination. The same process is repeated till k ($k \in [10, 150]$) frequency bands are kept. The ranking numbers are assigned during recursive elimination process and the frequency bands are ranked from high to low by importance.

4.3.4 Classifier training

Four traditional supervised classifiers are trained with the data of selected frequency bands, including SVM, KNN, DT, and linear SVM with SGD training. A total of 300 full band samples collected from each experimental scenario with and without human occupancy are randomly divided into training data set and testing data set. The training data is fed to each individual classifier and used to train the model accordingly. The input of each classifier is the list of average power of selected frequency bands and the list of the associated labels. Then these four models are trained individually for each

Table 6. Training setup for all scenarios and classifiers.

Scenario	# of Full Band Samples	# of Bands Selected	Classifier
StRmP1, … CrP3	[10, 20, … 60]	[10, 20, … 150]	SGD, SVM, KNN, DT

scenario based on each band selection result which are listed in Table 6. For example, for scenario StRmP1, 10 full band samples are randomly selected out of 150 full band samples of the occupied group and 10 full band samples are randomly selected out of 150 full band samples of the unoccupied group. The 10 most sensitive frequency bands are selected using these 20 full band samples. The average power of these selected 10 frequency bands of 90 occupied and 90 unoccupied samples is used to train all the classifiers. The same process is repeated for different number of full band samples and different number of selected bands as indicated in Table 6 to find the optimal setup. For each scenario, a total of 90 experimental runs are conducted for a classifier. Different percentage of training samples over total samples is also surveyed to identify the efficient training strategy.

4.4 Experimental Results

In order to quantify the overall accuracy of the occupancy detection result, the actual performance is evaluated by a confusion matrix with the same equations from (3.1) to (3.4). The F1 score is used this subsection to quantize the system performance unless otherwise specified.

4.4.1 Frequency bands selected

To find the optimal setup of the system, different numbers of full band samples and different numbers of selected frequency bands are tested. For the number of full band samples, from 10 to 150 samples with a step of 10 samples are tested. When each number of full band samples is tested, frequency bands from 10 to 60 bands with a step of 10 bands are selected and used for human detection. The same process is applied in all seven scenarios. PCA and RFE-LR are used for band selection individually and the corresponding selected features are used to train classifiers and detect occupancy. Figure 10 displays the results of bands selection of 2 different scenarios by the two different feature selection algorithms. The two scenarios are StRmP2 and CrP3. The subfigures in the left column display the rank of each frequency calculated by PCA and RFE-LR based band selection algorithms.

While the subfigures in the right column display the power spectrum marked with 30 selected frequency bands. The figures from Figure 10.a1 to b2 are for scenario StRmP2 and figures from Figure 10.c1 to d2 are for scenario CrP3. For example, Figure 10.a1 and b1 depict the rank of frequency bands evaluated by PCA and RFE-LR for the same scenario StRmP2 using 60 full band samples. The results in Figure 10 show that PCA and RFE-LR based algorithms produce similar ranking results. Figure 10.a2 and b2 are the band selection results of scenario StRmP2. The dark dots in these two figures represent the frequency bands selected. For better visualization, the zoomed in version of certain frequencies are displayed to compare the results of two band selection algorithms. The results show that sensitive frequency bands can be picked by both unsupervised and supervised algorithms. The frequency bands selected by the two algorithms are slightly different but have very similar clusters around 600MHz and 1100MHz. The ranking results and band selection results depend on locations and the spectrum variance caused by human body. Both band selection algorithms select the frequency bands where significant variation exists between the occupied and unoccupied spectrum. The results demonstrate that the developed adaptive sensing techniques can work as long as human subject has RF signatures in the SDR’s frequency range.

The cluster effect in the selected frequency bands can be detected in Figure 10 in different scenarios. Examples of selected frequency bands across all seven scenarios by PCA and RFE-LR are listed in Table 7. In these two examples, 10 frequency bands are picked by each algorithm from randomly selected 40 full band samples for 7 scenarios in the order from most significant to least significant in corresponding scenario with and without human occupancy 20 each class. The results show that there is at least one enclose cluster in each location. For example, in scenario StRmP1 and StRmP2 where data is collected in the study room, there are a few bands selected around 600MHz. The same can be observed in the bedroom and car locations. The cluster effect is shown in the results of both band selection methods. Another example, scenario CrP1, the frequency band selected are between 514.8MHz and 638.4MHz in both Table 7.a and b. Multiple frequency bands around 1100MHz are picked by PCA and RFE-LR in scenario StRmP2. Similar patterns are shown in other scenarios. The cluster effect could be related to the surrounding environment and antenna's direction and setup. The cluster effect can be used to establish a baseline of dynamic band selection because the selected frequency bands across all the three locations have common frequencies from 500MHz to 700MHz. Thus, less power will be required band selection time can be shortened. This cluster effect may also be useful for the study of human RF signature prediction. Electromagnetic and biological experiments can be designed to further investigate the cluster phenomenon.

The power of dynamically selected frequency bands data is used for HOD. In order to improve the system efficiency, the number of frequency band needed for

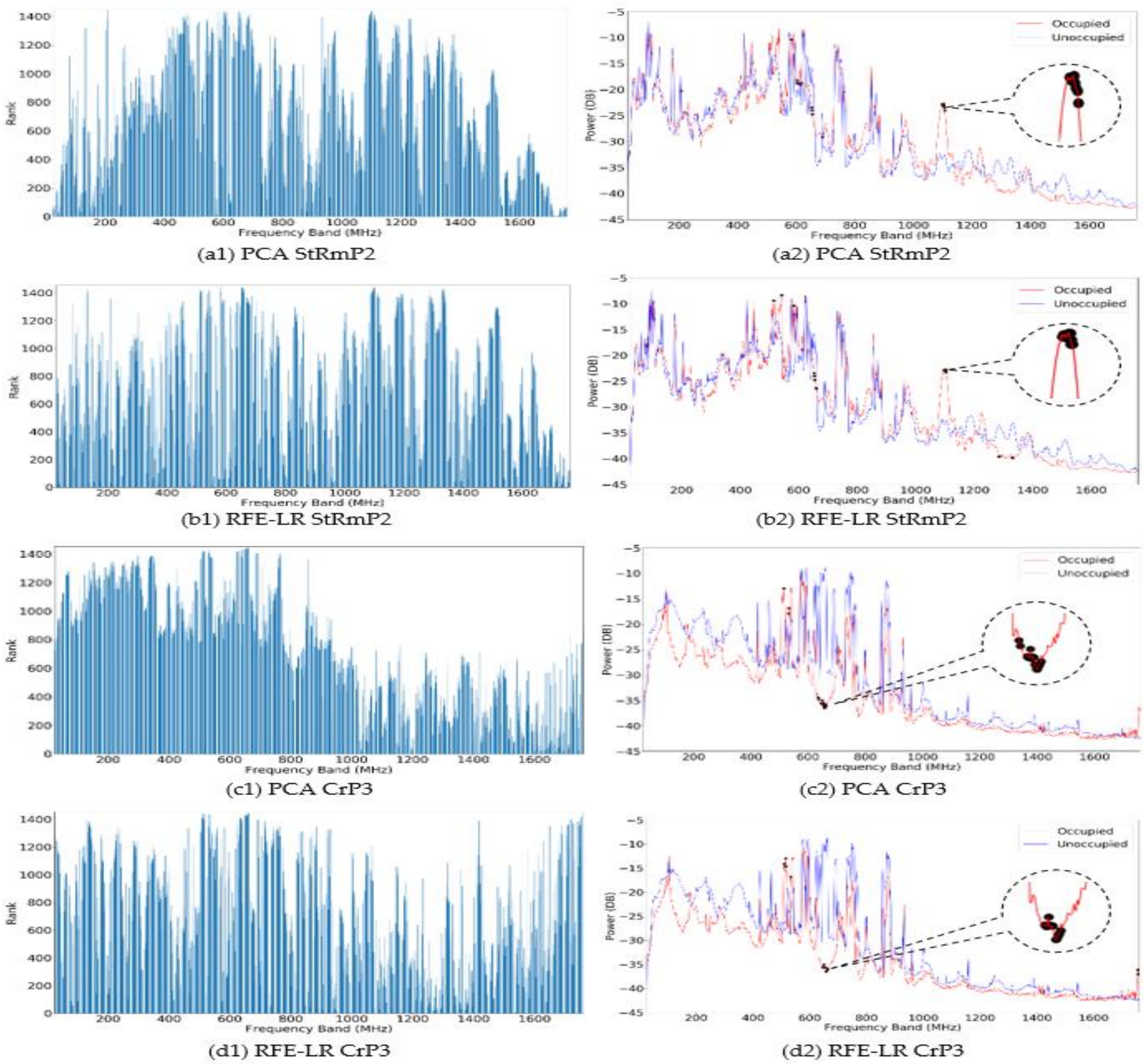

Figure 10. Examples of band ranking and selection results.

Table 7. The example of bands selection result.

(a) PCA

StRmP1 (MHz)	StRmP2 (MHz)	BdRmP1 (MHz)	BdRmP2 (MHz)	CrP1 (MHz)	CrP2 (MHz)	CrP3 (MHz)
180.0	206.4	1755.6	1755.6	637.2	517.2	531.6
930.0	1101.6	1758.0	1756.8	636.0	513.6	532.8
178.8	583.2	1756.8	1758.0	514.8	625.2	542.4
614.4	1102.8	1759.2	1759.2	537.6	626.4	646.8
603.6	1104.0	1754.4	621.6	516.0	624.0	645.6
612.0	1105.2	583.2	626.4	634.8	742.8	648.0
604.8	1100.4	582.0	625.2	538.8	741.6	534.0
602.4	1099.2	584.4	1754.4	638.4	740.4	537.6
177.6	654.0	580.8	622.8	584.4	692.4	649.2
176.4	614.4	452.4	624.0	633.6	693.6	636.0

(b) RFE-LR

StRmP1 (MHz)	StRmP2 (MHz)	BdRmP1 (MHz)	BdRmP2 (MHz)	CrP1 (MHz)	CrP2 (MHz)	CrP3 (MHz)
102.0	132.0	103.2	516.0	540.0	463.2	531.6
206.4	583.2	109.2	517.2	541.2	464.4	532.8
216.0	654.0	486.0	552.0	542.4	583.2	645.6
396.0	660.0	488.4	553.2	580.8	597.6	649.2
505.2	1098.0	544.8	554.4	582.0	618.0	658.8
513.6	1099.2	595.2	649.2	583.2	764.4	660.0
649.2	1100.4	624.0	650.4	634.8	768.0	661.2
650.4	1101.6	633.6	655.2	636.0	770.4	662.4
1335.6	1285.2	798.0	660.0	637.2	798.0	1755.6
1336.8	1286.4	858.0	661.2	638.4	960.0	1756.8

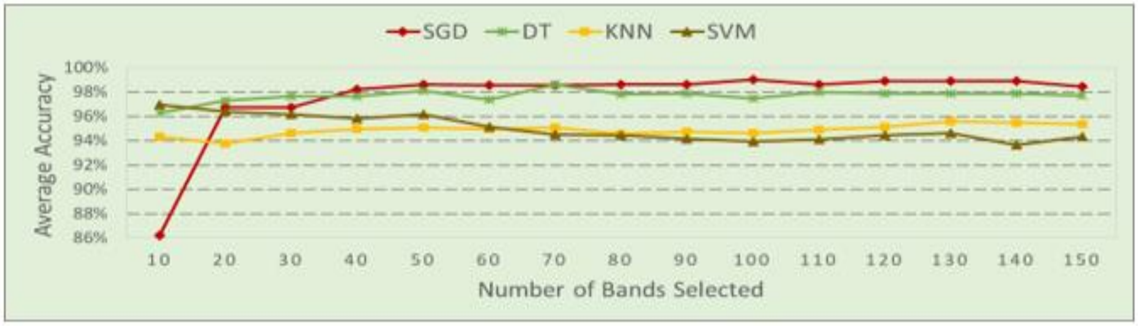

(a) PCA

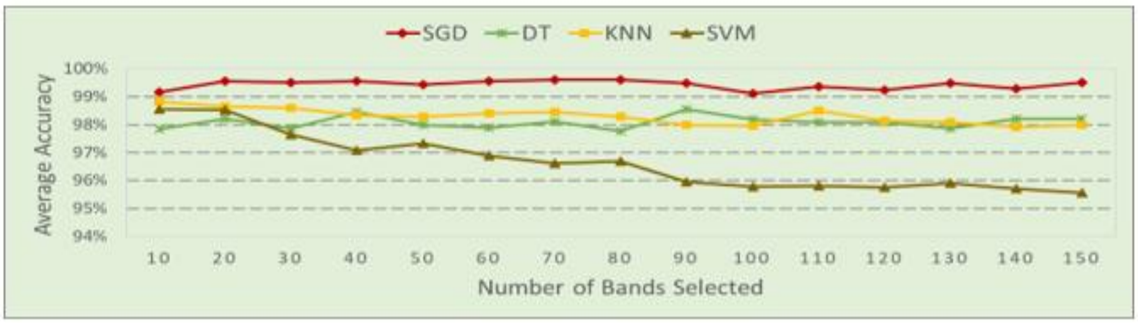

(b) RFE-LR

Figure 11. Accuracy vs the number of bands used.

detection is evaluated. The average occupancy detection accuracy of each classifier by using frequency band selected by each band selection method is depicted in Figure 11. In the figure, average accuracy is calculated by corresponding F1 score recorded during each experimental run. Let M be the number of steps of full band samples and a which is the F1 score of each experimental run, the average accuracy of each scenario is calculated by $ds_{avg} = (\sum_{i=1}^{M} d_i)/M$. The average accuracy of each classifier of each band selection algorithm is calculated by $dc_{avg} = (\sum_{i=1}^{L} ds_{avg})/L$, where L is the number of scenarios. The experiment results displayed in Figure 11 indicate that optimal feature selection policy could improve the system efficiency. The detection accuracy increases with the number of selected bands initially, then maintains at the same level or drops slightly after certain number of bands selection. For example, by using band selection algorithm PCA, the classification accuracy of model SGD increases from 86% to 98% when the number of frequency bands increases from 10 to 40. There is very limited improvement when more frequency bands are used. So, 40 can be regarded as a cutoff number in band selection by SGD. DT shows a similar trend but performs slightly worse after 70 frequency bands. The SVM works the best using only 10 bands and the performance drops continually afterwards. KNN shows improvements from 10 to 40 bands and slowly deteriorates after that. Similar trends are shown in the results of RFE-LR, but the cutoff number can be different. SGD reaches the best performance at 20 bands. DT learning does not have significant improvement after 40 bands. The performance of KNN and SVM continually drops after 10 bands. When only 10 frequency bands are scanned by the SDR, nearly 97.2% energy and time can be saved comparing to using the 1447 full bands data.

We have also investigated how the number of full band samples affects band selection and the classifiers' accuracy. The results are shown in Figure 12. F1 score is used to calculate the average accuracy with similar process above. Let N be the number of bands selected. d is the F1 score obtained in each experiment. The average accuracy of each scenario is calculated by $ds_{avg} = (\sum_{i=1}^{N} d_i)/N$. The average accuracy of each

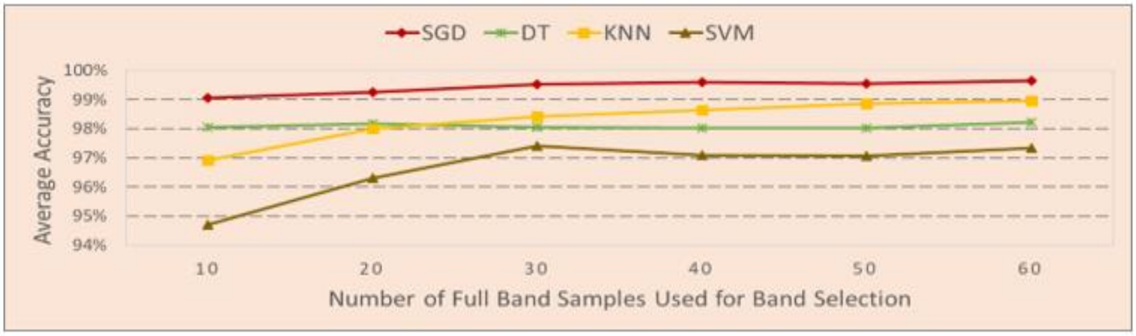

(a) PCA

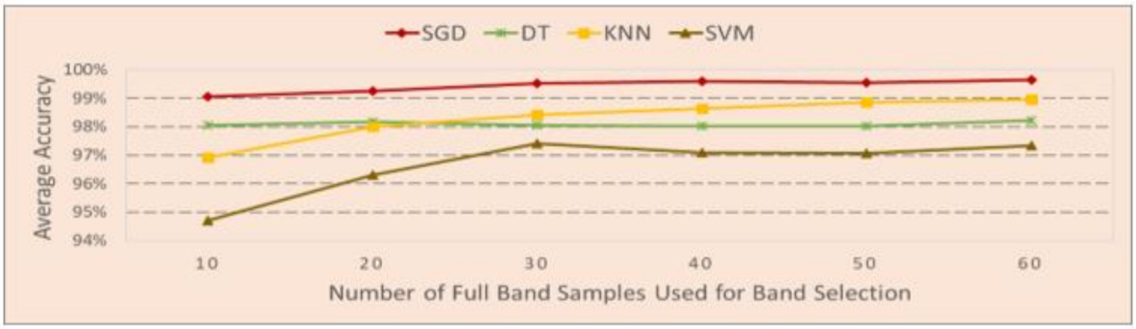

(b) RFE-LR

Figure 12. Accuracy vs number of samples for bands selection.

classifier of each band selection algorithm is calculated by $dc_{avg} = (\sum_{i=1}^{L} ds_{avg})/L$, where L is the number of scenarios. In Figure 12.a, the overall trend shows that the performance increases when the number of frequency band samples used for band selection increases from 10 to 20 bands and the accuracy of all four classifiers saturates after the cutoff number of 20 by PCA based band selection. However, in Figure 12.b, which is through RFE-LR based band selection method, classifiers SGD and SVM reach the best performance at 30 samples and KNN shows continuous improvement till 60 samples. DT is not very sensitive to the number of samples for band selection. The

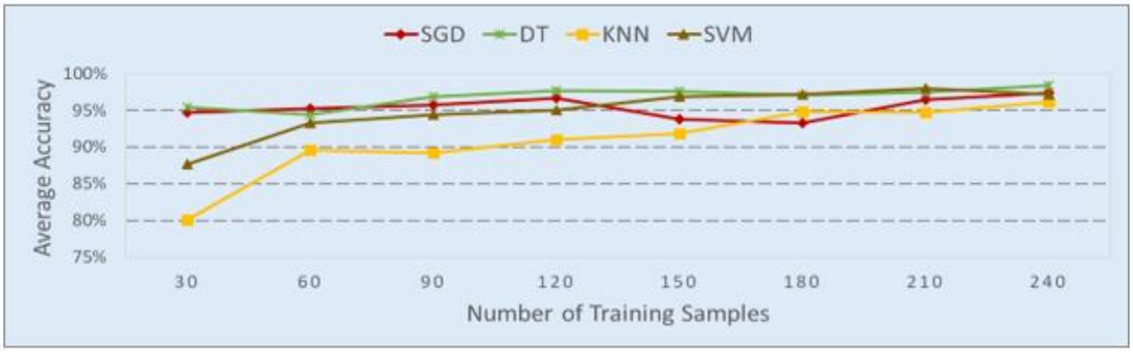

(a) PCA

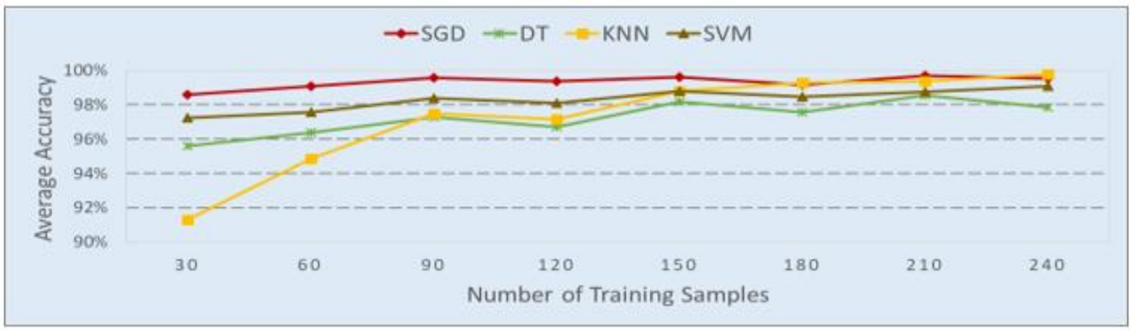

(b) RFE-LR

Figure 13. Accuracy vs. number of samples for classifier training.

overall trend in these Figure 6 indicates that a very large number of full band samples used for band selection does not help in most situation and building an online training system is feasible with as little as 20 to 30 full band samples.

The number of samples to train the classifiers is studied and the results are shown in Figure 13. In this study, 60 full bands samples including 30 in occupied group and 30 in unoccupied group are used for band selection. 20 frequency bands are selected by PCA and REF-LR based algorithms from the same frequency data samples in each scenario. The number of samples used to train the classifiers varies from 30 to 240. The F1 score is used to calculate the average accuracy. Let L be the number of scenarios and$a$be the F1 score of each experiment. The average accuracy of each classifier is calculated by $ds_{avg} = (\sum_{i=1}^{L} d_i)/L$. Each classifier shows a similar trend where classifier's performance improves with the increase of training samples except DT with PCA based band selection method. In that case, the number of training samples does not have a significant impact to the classifier's performance. For classifiers SGD, DT and SVM, these are not significant improvement of accuracy or it gets a little worse after cutoff number 90. KNN requires 180 training samples to achieve the best performance.

4.4.2 Performance in different locations

We compare the classifier's performance in different locations in this subsection. Table 8 lists the precision, recall, F1 score and accuracy of SGD in different locations. In this example, 20 frequency bands are selected by PCA or RFE-LR from 60 full band samples, 30 in each occupancy status, in each perspective scenario. Classifier SDG is trained to detect human occupancy. RFE-LR based band selection achieves better overall system performance. The detection results from the other three classifiers also indicate that RFE-LR based band selection can lead to better detection performance.

An example of all the classifiers' performance at different locations is presented in Table 9. In this example, 30 frequency bands are selected by PCA or RFE-LR based algorithms from 80 full band samples, with 40 in each occupancy status, in each perspective scenario. 60% of the collected samples are used to training and the rest are used for testing. Other experiments with different number of frequency band selected and different number of full band samples used for band selection yield similar results.

Table 8. The performance of stochastic gradient descent model.

(a) PCA

Scenario	Precision	Recall	F1	Accuracy
StRmP1	98.33%	98.33%	98.33%	98.33%
StRmP2	100.00%	100.00%	100.00%	100.00%
BdRmP1	91.67%	91.67%	91.67%	91.67%
BdRmP2	100.00%	100.00%	100.00%	100.00%
CrP1	100.00%	100.00%	100.00%	100.00%
CrP2	96.61%	95.00%	95.80%	95.83%
CrP3	100.00%	100.00%	100.00%	100.00%

(b) RFE-LR

Scenario	Precision	Recall	F1	Accuracy
StRmP1	100.00%	100.00%	100.00%	100.00%
StRmP2	100.00%	96.67%	98.31%	98.33%
BdRmP1	100.00%	96.67%	98.31%	98.33%
BdRmP2	100.00%	100.00%	100.00%	100.00%
CrP1	100.00%	100.00%	100.00%	100.00%
CrP2	100.00%	98.33%	99.16%	99.17%
CrP3	100.00%	100.00%	100.00%	100.00%

Table 9. The classifiers' performance at different locations.

(a) PCA

Scenario	SGD	DT	KNN	SVM
StRmP1	90.48%	95.65%	90.09%	100.00%
StRmP2	100.00%	100.00%	99.16%	100.00%
BdRmP1	93.75%	96.67%	87.80%	92.31%
BdRmP2	100.00%	100.00%	100.00%	100.00%
CrP1	100.00%	100.00%	100.00%	94.49%
CrP2	96.67%	98.31%	92.86%	95.24%
CrP3	100.00%	100.00%	100.00%	97.56%

(b) RFE-LR

Scenario	SGD	DT	KNN	SVM
StRmP1	99.17%	92.56%	91.89%	98.36%
StRmP2	100.00%	99.16%	100.00%	100.00%
BdRmP1	100.00%	97.52%	100.00%	100.00%
BdRmP2	100.00%	100.00%	100.00%	100.00%
CrP1	98.31%	100.00%	100.00%	96.77%
CrP2	100.00%	91.89%	97.44%	96.00%
CrP3	100.00%	100.00%	100.00%	96.77%

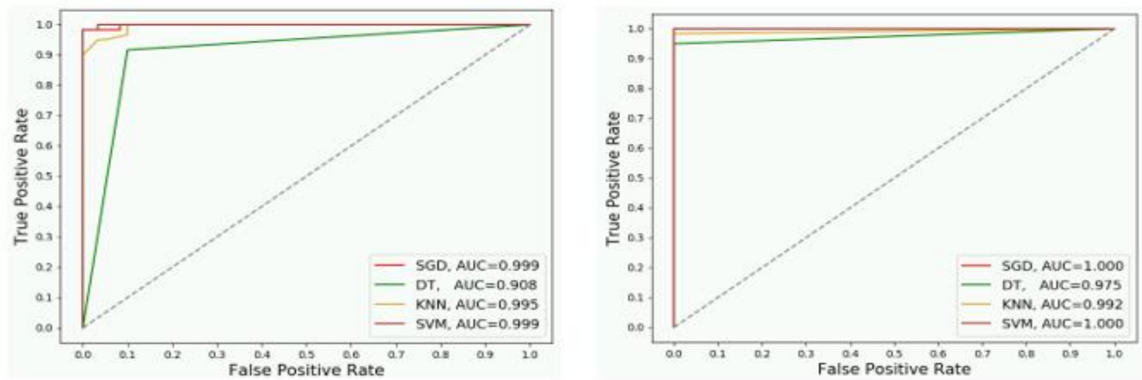

(a) PCA (b) RFE-LR

Figure 14. Receiver operating characteristic curve.

4.4.3 Performance by different band selection algorithms

We evaluated how band selection algorithm affects the classifiers' accuracy. The detection rate and false alarm rate are measured during the experiment. The receiver operating characteristic (ROC) curves of all four classifiers are displayed in Figure 14 correspond to PCA and RFE, separately, to select 40 frequency bands from 40 full bands samples in scenario StRmP1. The area under the curve (AUC) in these two figures indicated that classifiers perform better using REF selected frequency bands except KNN shows slightly lower performance.

F1 score is used to calculate the average accuracy at different locations which is shown in Figure 15. Let N be the number of experiments executed for each scenario which value is 90. a is the F1 score obtained in each experiment run. The average accuracy of each scenario of each band selection algorithm in Figure 15.a and Figure 15.b is calculated by $ds_{avg} = (\sum_{i=1}^{N} d_i)/N$. The average accuracy of each classifier of each

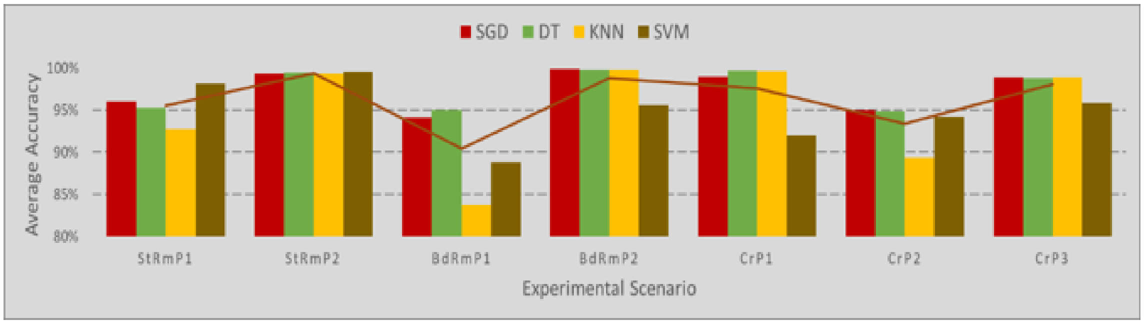

(a) PCA

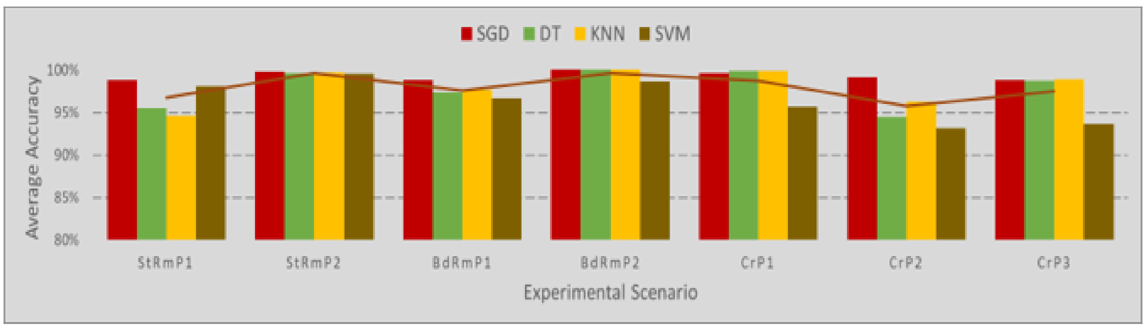

(b) RFE-LR

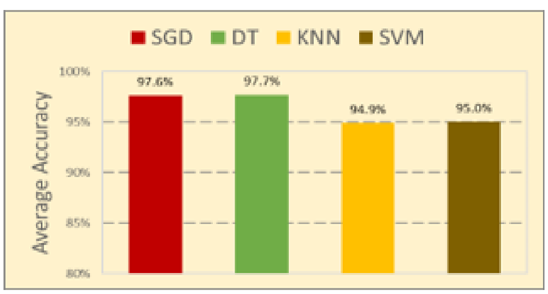

(c) PCA

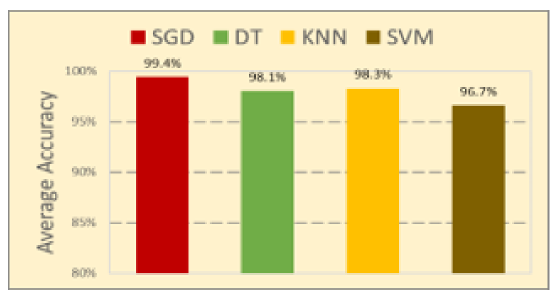

(d) RFE-LR

Figure 15. Average accuracy of human detection.

band selection algorithm in Figure 15.c and Figure 15.d is calculated by $dc_{avg} = (\sum_{i=1}^{L} ds_{avg})/L$, where L is the number of scenarios. The average detection accuracy in each scenario in Figure 15.a and Figure 15.b shows similar results studied in subsection 4.2.2. Using the frequency bands selected by RFE-LR, the detection accuracy of each classifier achieves better result in most scenarios. More clear results are directed in Figure 15.c and Figure 15.d. With the help of RFE-LR the average accuracy of KNN is improved by 3.4% from 94.8% to 98.2% and rest three classifiers also show increments.

RFE-LR band selection algorithm helps all four classifiers to achieve better results which is also higher than the accuracy of 95% obtained by CNN in our research in phase one. The highest performance is obtained by SGD using frequency bands picked by RFE-LR. The system performance can be improved by smartly choosing the dynamic band selection algorithm, the classifier and other parameters such as the number of band selected, number full band samples used for band selection and the number of samples used to train the model. Figure 8 summarizes all the studies presented in the thesis for passive RF HOD.

4.4.4 Storage and processing evaluation

The system's storage and processing needs are also evaluated as the final goal of this research work is to implement all the functions on an embedded system. In the case of selecting 30 frequency bands from 60 full band samples, and processing data on a single core of central processing unit (CPU) ‘AMD Ryzen Threadripper 2950X 16-Core Processor’, 70.5M bytes of memory are used, and 2.74% processor is utilized by PAC; Using RFE consumes 65.2M bytes memory and the processor utilization rate is 2.89%

with the same case and on the same processor. So, we believe the system's storage and processing needs can be fulfilled by a well-designed embedded system.

4.5 Summary

A new efficient, low cost and environment friendly solution is proposed to detect human occupancy in enclosed spaces via passive CR. The solution is based on reconfigurable software defined radio system and adaptive spectrum sensing technology. The experiment results show that CRhodora system is capable of accurately detecting human occupancy not only in residential rooms but also in commercial vehicles under different settings such as various distances between the human subject and the antenna. Frequency bands sensitive to human occupancy can be determined by both unsupervised and supervised dynamic feature selection algorithms. The supervised RFE-LR based algorithm shows an improvement in performance over to the unsupervised PCA based algorithm. The accuracy of occupancy status estimated by traditional classifiers trained on selected significant features surpass the CNN on this task through the help of adaptive spectrum sensing technology. By dynamically configuring CR and adaptively sensing the spectrum at the location of interests, the overall speed and power consumption is improved by 97.2%.

This investigation reveals some interesting phenomenon, such as the clustering of frequency bands sensitive to human body around 600MHz, which requires a more thorough study. We are particularly interested in synthesizing human RF signatures for a given baseline spectrum. Such a capability to predict human RF signatures can be very useful in both security and smart building applications. GAN is widely used for synthesizing related signatures and is explored in phase three.

CHAPTER FIVE

SYNTHESIS OF HUMAN RADIO FREQUENCY SIGNATURES

5.1 Introduction

Adversaries can easily jam a wireless environment by emitting interference RF signals or simply replaying the recorded data. A passive RF signals-based security monitoring system should have the awareness of the RF environment to maintain its reliability and robustness. RF environments vary with locations. Thus, the system should easily adapt to a new environment with minimum user effort through synthesis of human RF signatures after measuring the baseline spectrum of the new environment. The knowledge of spectrum variation caused by human occupancy and synthesizing human RF signatures are critical aspects of building a more efficient, robust, and secure real-time indoor monitoring system. An open question this thesis addresses is whether this variation can be synthesized. GAN are powerful tools which can learn from labeled samples and generate features based on the knowledge gained. A HSGAN model synthesizes passive RF signals with human occupancy via the baseline spectrum without human occupancy collected in the enclosed space is developed in phase three.

5.2 Advantages

We propose a HSGAN model which generates the RF signals from the baseline spectrum at the location of interest. There are several advantages offered by the HSGAN approach: (1) through proactively predicting the wireless environment at the location of interest, the passive RF based HOD system is capable of recognizing the spoofing or jamming signals which are used to disturb ambient spectrum from the real human RF signatures; (2) the passive RF based HOD system can fit a new spectrum circumstance easier without retaining the classifier. It enhances flexibility of the system and the maintenance coast is reduced; (3) through bands selection strategy, only the signals containing important information are synthesized from which the efficiency of the system is increased.

5.3 Technical Approach

The human RF signatures synthesis system is built in our experiment and is depicted in Figure 16. The system includes a receiving antenna, an SDR, a data reprocessing module, a band selection module, and a HSGAN module. The RF signals are collected from enclosed spaces. In the initial stage, the SDR is configured to scan the whole spectrum in its frequency range (24-1760 MHz). Meanwhile, the collected data is

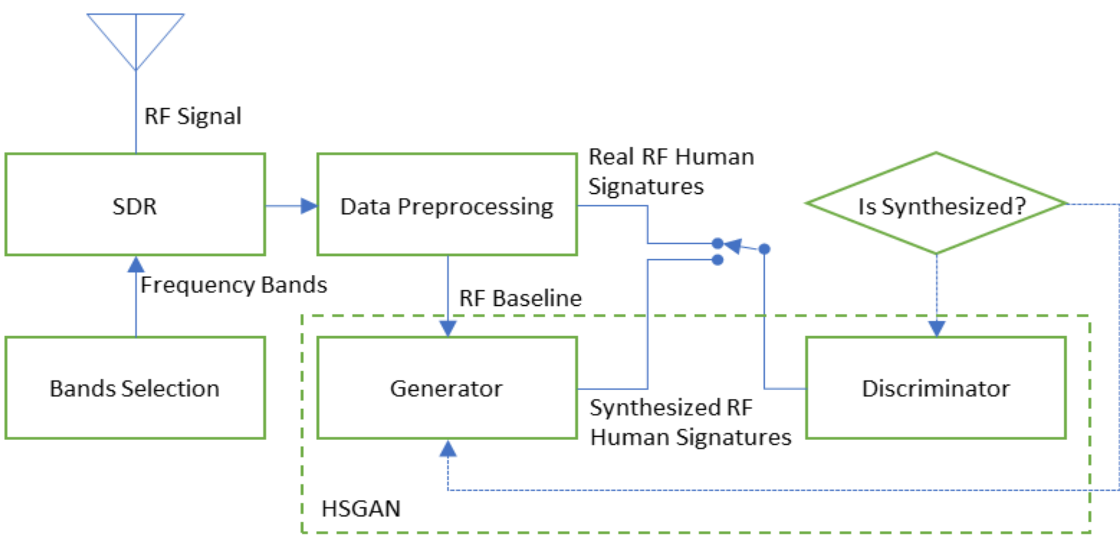

Figure 16. Signature synthesis system.

automatically labeled, and the collected RF signals corresponding to the human occupancy status are associated to the labels. After enough whole spectrum samples are collected, the frequency bands which are sensitive to HOD are selected. Then, only the selected frequency bands are scanned by the reconfigured SDR. The HSGAN including a generator and a discriminator are trained with the baseline spectrum and the human RF signatures in the selected frequency bands. The generator synthesizes the RF human signals to simulate the spectrum when the enclosed space is occupied. Lastly, a CNN model and a KNN model are trained with the real signals in the selected frequency bands with and without human occupancy at the location of interest. The performance of human RF signatures synthesis system is evaluated by the classification results of the trained CNN and KNN models taking the inputs of the real baseline spectrum and the synthesized RF data. The signal acquisition and pre-processing are introduced in subsection 5.1.1 and 5.1.2. Subsection 5.1.3 illustrates the frequency bands selection algorithm. Finally, the structure of HSGAN, the training process and evaluation methods are presented in Subsections 5.1.4, 5.1.5, and 5.1.6.

5.3.1 RF signal Acquisition

The data collection is the similar to the data collection in phase one described in Table 1 at each experiment location, the study room and the office except that only full band is scanned. A full band sample refers the frequency data collected through a scan from the lowest frequency to the highest frequency. One full band sample has 1447 frequency bands' raw data. A total number of 1296 full band samples with human occupancy and an equal number of samples without human occupancy were randomly collected in the study room from 6 am to 10 pm across 3 months to eliminate the impact of spectrum variation among different timeframes in the day. 879 full band samples with human occupancy and equal number of samples without human occupancy were collected in the office with the same strategy.

$p(f)$ is the average power of frequency band centered at f and is used throughout the experiment. It is calculated using the same equation (2.1).

5.3.2 Frequency Band Selection

The $p(f)$ in the power spectrum is used to select the bands sensitive to HOD. In this research work, the PCA algorithm with 1447 $p(f)$ as the input features is applied to extract the principal components. Frequency bands according to their values in the extracted components are selected. It is not suggested to directly use the extracted principal components as the features because subsequent spectrum sensing still has to involve all of the frequency bands, since each principal component is a linear combination of all the original frequency bands [63]. According to the measurement variance, the principal components are ranked from high to low by the importance after they are extracted. Then, the first three components are kept. Lastly, k ($k = 784$) frequency bands are selected which have the highest absolute coefficients in the first three components.

5.3.3 Human Signature Generative Adversarial Networks

A GAN is a framework proposed by Goodfellow et al. [64] which estimates the generative mode via an adversarial process. During the GAN process, two models including a discriminator D and a generator G are trained simultaneously. The data distribution under estimation is captured by the generator G. The generative model G generates fake samples through its captured distribution. The fake samples and real training data are fed to the discriminator D which classifies if the input samples come from the training data rather than generated by G. The training process is a two players' game. The goal of G is to maximize the probability of D to make the mistakes and the goal of D aims to minimize its chances to be fooled by G. In HSGAN, the human RF signatures are synthesized via the baseline spectrum. The discriminator loss $\mathcal{L}_D$ and the generator loss $\mathcal{L}_G$ are defined as follows:

$$\mathcal{L}_D = E_{p(f_{ok}) \sim P_{data}(p(f_{ok}))}\left[log\, D\big(p(f_{ok})\big)\right] + \quad E_{p(f_{uk}) \sim P_{p(f_{uk})}}\left[log\left(1 - D\left(G\big(p(f_{uk})\big)\right)\right)\right] \tag{5.1}$$

$$\mathcal{L}_G = E_{p(f_{uk}) \sim P_{p(f_{uk})}(p(f_{uk}))}\left[log\left(D\left(G\big(p(f_{uk})\big)\right)\right)\right] \tag{5.2}$$

The number of k average powers with and without human occupancy are extracted from the selected k frequency bands are denoted by $p(f_{ok})$ and $p(f_{uk})$ respectively. $P_{data}\big(p(f_{ok})\big)$ is the probability distribution over $p(f_{ok})$ and $P_{p(f_{uk})}\big(p(f_{uk})\big)$ is the probability distribution over $p(f_{uk})$. G estimates the human RF signatures probability distribution over the input of $p(f_{uk})$. The training is defined as:

$$\max_{D} \min_{G} C(G; D) = \mathcal{L}_D \tag{5.3}$$

The generated data $G\big(p(f_{uk})\big)$ from G and real sample $p(f_{ok})$ are fed to D. D estimates the probability of its input is $G\big(p(f_{uk})\big)$ rather than $p(f_{ok})$. The cost function $C(G; D)$ depends on both the generator G and the discriminator D. The calculated loss $\mathcal{L}_D$ is propagated back to update both G and D. G maximizes $\mathcal{L}_D$ and D minimizes $\mathcal{L}_D$. The G is optimal when the D cannot distinguish $G\big(p(f_{uk})\big)$ from $p(f_{ok})$. The D is optimal when the D can recognize $p(f_{ok})$ from generated $G\big(p(f_{uk})\big)$. The process repeats till both models are optimized.

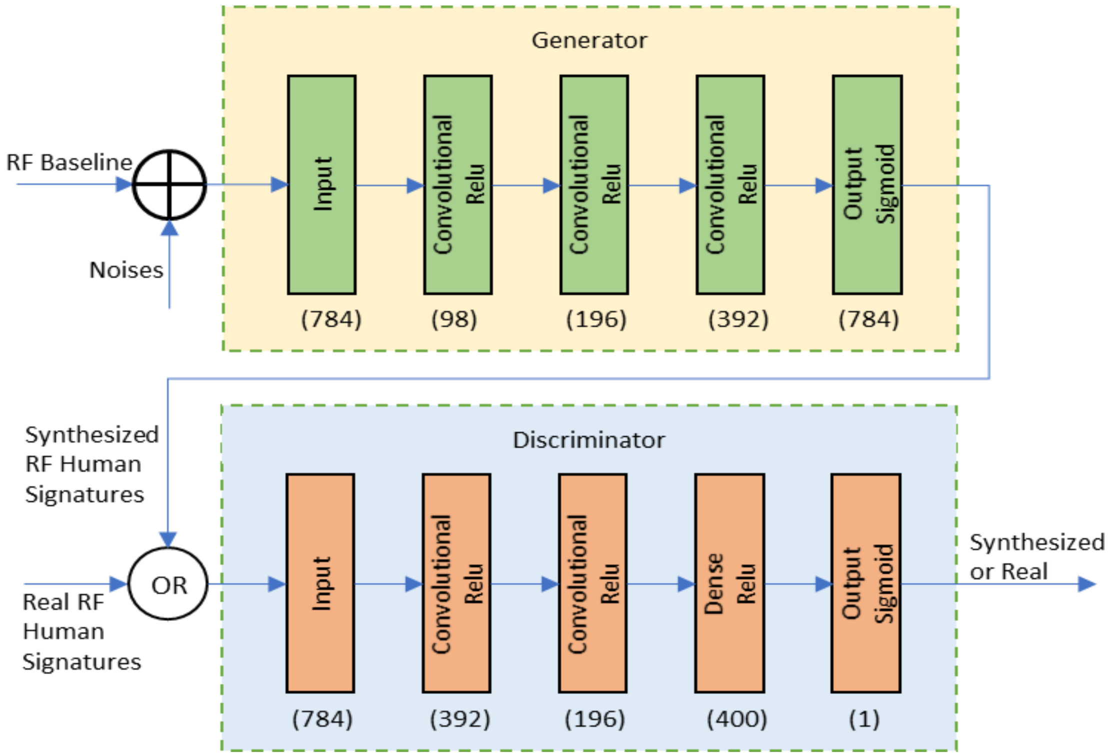

Figure 17. Generative model structure.

Both mode G and D are CNNs and their designs are displayed in Figure 17. G has total 5 layers including one input layer, three convolutional layers and one output layer. The number of neurons and activation functions of each layer are displayed in Figure 17. Similarly, D has 5 layers including one input layer, two convolutional layers, one dense layer and one output layer. The number of neurons and activation functions of each layer are also displayed in the figure.

5.3.4 HSGAN Model Training

These extracted $p(f_{ok})$ and $p(f_{uk})$ from the power spectrum collected are randomly selected as the training and validation samples. These samples are used for

HSGAN model fitting and evaluation. Only the samples of the study room are used to train the HSGAN model. The trained HSGAN model generates k average powers to simulate human RF signatures which is donated as $p(f_{sok})$. Each value in the samples is normalized before fitting the model and the normalized data range is from 0 to 1. Uniformly distributed noise ranging from -0.0001 to 0.0001 is added to each value in the training sample in order to improve the model's generalization from which the sample is fed to G. The outputs from generator, of $p(f_{sok})$ and $p(f_{ok})$ in the training sample, are fed to D alternately. The Adam optimizer is used during training, the learning is 0.0002, beta1 is 0.5, beta2 is 0.999 and epsilon is 1e-8. Batch size is 4 and total 90 epochs is trained till both Gand D are optimized.

5.3.5 HSGAN Model Evaluation

In order to evaluate the performance of HSGAN model, two classifiers including a CNN and a KNN are built to take the input of generated $p(f_{sok})$ and $p(f_{uk})$ to estimate occupancy status. To build these two classifiers, CNN and KNN models are trained with the real data, $p(f_{uk})$ and $p(f_{ok})$ of the study room and corresponding labels, where the number of training samples are 70% of the number of collected samples of each occupancy status, which is 907 out of 1296. The rest 389 samples of each occupancy status are used for testing which are unseen during the training of CNN and KNN. The number of 1296 samples of $p(f_{sok})$ are synthesized by G taking the input of $p(f_{uk})$ of the study room which is added by uniformly distributed noises ranging from -0.0001 to 0.0001 before being fed to G. Then, the generated 1296 samples of $p(f_{sok})$, including the 389 samples of $p(f_{uk})$ and corresponding labels, are fed to trained CNN and KNN models for classification. Similarly, the number of 879 $p(f_{sok})$ are synthesized using the data $p(f_{uk})$ of the office scene are evaluated by CNN and KNN models. These two trained classifiers should be able to accurately distinguish the occupancy status, and the classification results indicate the performance of our proposed HSGAN. Apart from these two classifiers, the correlation between generated data and real data is also calculated for evaluation.

5.4 Experimental Results

In order to quantify the overall accuracy of the occupancy detection result, the actual performance is evaluated by a confusion matrix with the same equations from (3.1) to (3.4). The F1 score is used this subsection to quantize the system performance unless otherwise specified.

5.4.1 Synthesized human RF signatures

Figure 18 depicts examples of synthesized human RF signatures and baseline spectrum at the location of study room. Figure 18(a) presents an example of the average powers in the selected 784 frequency bands generated by HSGAN model using baseline spectrum when the study room is unoccupied and Figure 18(b) is a real sample of human signatures collected when the study room is occupied. The overall trends of these two samples are similar and the peaks appear at similar frequency bands such as 0.1 GHz, 0.2 GHz, 0.37 GHz, 0.48 GHz, 0.69 GHz, and so on. The two samples have valleys at similar frequencies as well.

A total number of 1296 samples of human RF signatures are generated from 1296 samples of baseline spectrums. To better examine the synthesized signals, the average

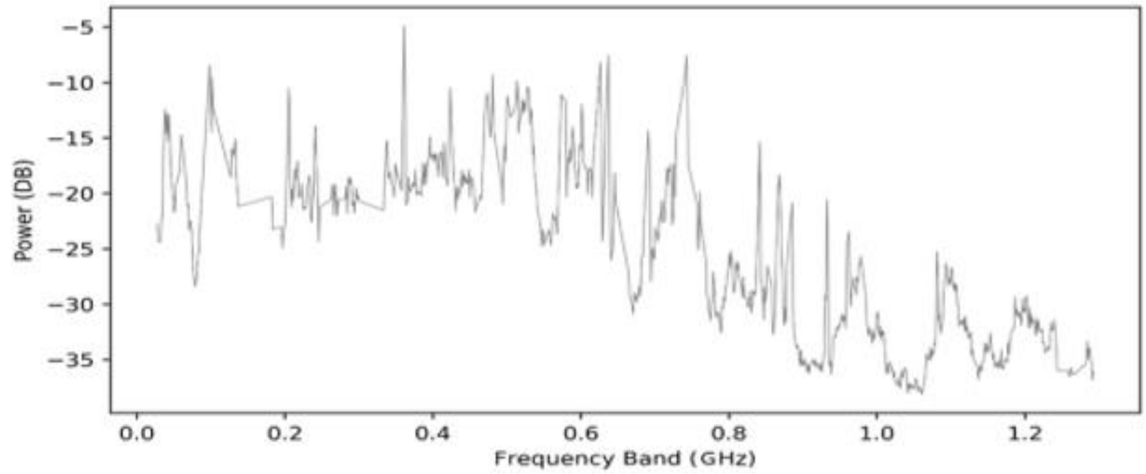

(a) Synthesized

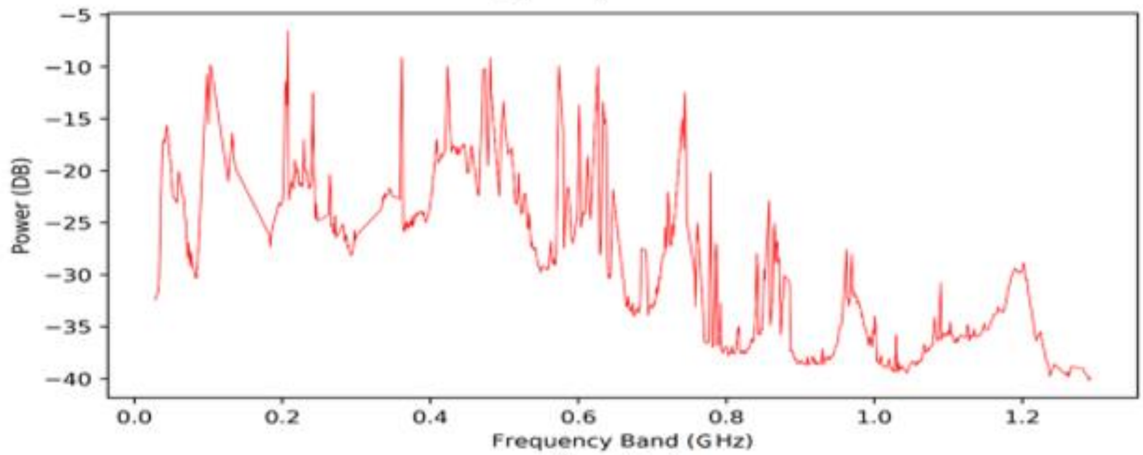

(b) Real

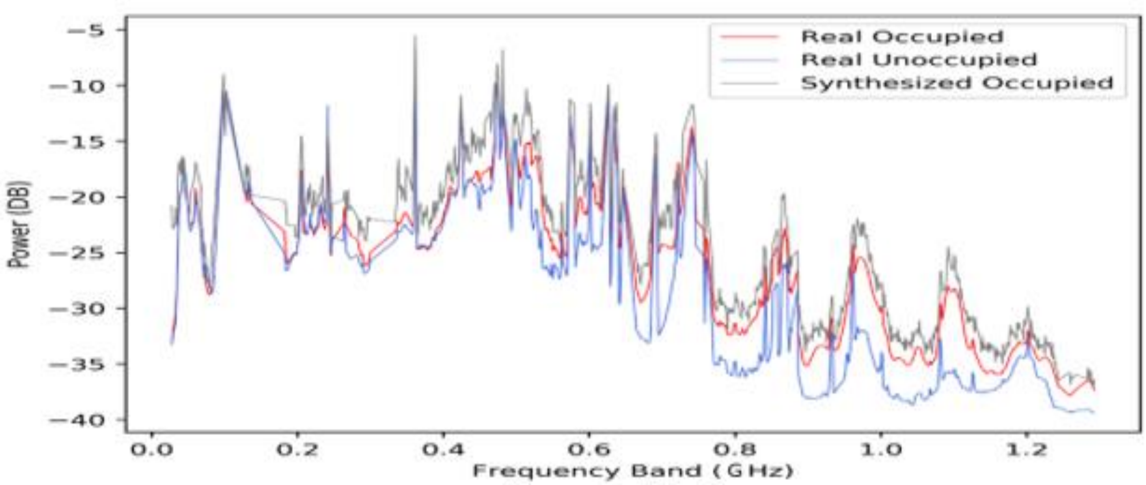

(c) Combined

Figure 18. Synthesized human signature.

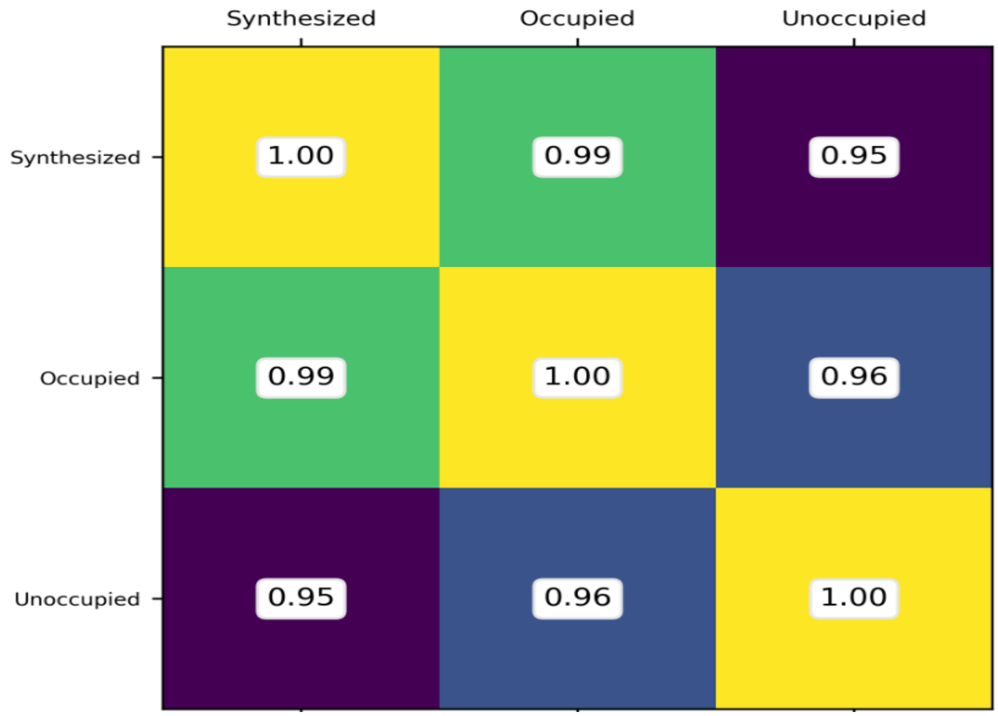

Figure 19. Correlation of synthesized data and real data.

signals with human occupancy, the blue line is the baseline spectrum and the gray line is synthesized. The red line and gray line are closer in the gaps in most frequency bands, especially the bands from 0.48 GHz to 1.3 GHz. However, in the lower frequency bands below 0.48 GHz, an opposite relationship is obtained. The synthesized signals are slightly above the real signal with human occupancy in the frequency bands higher than 0.17 GHz but almost overlap in the bands lower than 0.17 GHz. Further investigation is needed to study the reasons so that model enhancement can be made.

The correlation between the generated RF data and the real signals with human occupancy, and the correlation between the real signals with human occupancy and without human occupancy are shown in Figure 19. The correlation is calculated using the

1296 generated samples collected with and without human occupancy in the study room. The real occupied signals have a closer relationship with the generated signals as determined by the correlation between the real occupied signals and real unoccupied signals which is consistent with the visual observation.

5.4.2 Evaluation via detection results

Besides visually surveying the generated signals and calculating the correlation between the generate data and the real data evaluates the HSGAN. The CNN and KNN classifiers are trained with the real collected data with and without human occupancy in the study room. Then, these two trained models take the inputs of synthesized data and baseline spectrum of study room or office, respectively. The detection results of each model at each location are listed in Table 10. Both models and locations achieve very encouraging detection performance. The proposed HSGAN not only predicts the human RF signatures at the location of the RF signals in the study room, but also can generate the human RF signatures for a different location using the baseline spectrum at the new location, e.g., the office specifically, as a form of transform learning or domain adaptation.

5.5 Summary

Phase three presents a human RF signatures synthesis system using a GAN. The generated RF data by the system simulates the wireless signals in the enclosed space where is occupied by the human subject using the baseline spectrums without human occupancy. The system is based on the GAN model and reconfigurable software defined radio technology. The experimental results show that the proposed HSGAN model is not only capable of predicting the human RF signatures using the baseline spectrum at the trained location but also it can produce human RF signatures using the baseline signals at a new location without training. The synthesized RF data is evaluated quantitatively by CNN and KNN classifiers which are trained using the measured spectrum with and without human occupancy in the enclosed space. When fed with synthesized data and measured baseline spectrum, both classifiers produce HOD accuracy above 98 percent.

Table 10. Detection results of synthesized human RF signatures.

Location	Model	Precision	Recall	F1	Accuracy
Study Room	CNN	100%	99.92%	99.96%	99.94%
Study Room	RNN	98.33%	100%	99.16%	98.69%
Office	CNN	99.77%	99.43%	99.60%	99.39%
Office	RNN	98.98%	99.66%	99.32%	98.95%

CHAPTER SIX

SUMMARY

6.1 Conclusion

This thesis provides a complete, low-cost and green human occupancy detection (HOD) solution via passive radio frequency (RF) data through cognitive radio (CR) in the enclosed spaces. The throughout studies are conducted.

First, we survey the feasibility of HOD via passive RF data using convolutional neural network (CNN) in the residential study room and an office in the six-story building. Human occupancy is detected by passive RF wireless signals via deep learning neural network successfully. Testing against different frequency bands, locations and time periods indicates the robustness of this approach.

Second, in order to improve the efficient and reduce the energy consumption, an advanced CR HOD over RF analysis (CRhodora) system is set up and the adaptive spectrum sensing technology is utilized. Furthermore, the experimental scope is extended to include commercial vehicles in the enclosed spaces. Both unsupervised and supervised dynamic feature selection algorithms are capable of determining frequency bands sensitive to human occupancy. With the help of adaptive spectrum sensing technology, the accuracy of occupancy status estimated by traditional classifiers trained on selected significant features surpass the CNN on this task. By dynamically configuring passive CR and adaptively sensing the spectrum at the location of interests, the overall speed and power consumption is improved by 97.2%.

Third, to answer the question of whether the passive RF signals variation caused by human occupancy in the enclosed spaces can be synthesized, a human signature generative adversarial networks (HSGAN) model is proposed to synthesize passive RF data via the baseline spectrum without human occupancy collected in the enclosed spaces. The experimental results show that the proposed HSGAN model is not only capable of predicting the human RF signatures using the baseline spectrum at the trained location but also it can produce human RF signatures using the baseline signals at a new location without training. The synthesized RF data is evaluated quantitatively by CNN and k-nearest neighbors (KNN) classifiers which are trained using the measured spectrum with and without human occupancy in the enclosed space. When fed with synthesized data and measured baseline spectrum, both classifiers produce HOD accuracy above 98 percent.

6.2 Future Work

Our system shares some common characteristics of passive radar system and both systems are used for surveillance through object detection. No dedicated transmitters are required by these two systems since passive RF signals emitted by third parties are the sources. Without sending out signals, either system is difficult to be detected or tracked. Other benefits also come with this property of only receiver being required, for instance, the device size is smaller, and it is easier to deploy. Passive radar was invented in 1930s and revived in the 1980s with the rising of inexpensive computation power and receiver. Deep learning is also adopted by some research works in the field of passive radar recent years, but it has not been applied for HOD per our current literature study. Till now, HOD via passive RF data without depending on specific types of wireless signals is still a new research area and the publications are limited. To the best of our knowledge, other HOD via passive RF signal solution which does not relay on the specific types of RF signals has not be published. There are many research fields can be covered in the future.

First of all, different features of the RF signals such as the phase, amplitude, Doppler and received signal strength (RSS) instead of raw data can be utilized to estimate the human occupancy status in the enclosed spaces. Experiments using phase and amplitude have been carried out in our research work phase one and achieved similar accuracy comparing to using raw data. Features of Doppler and RSS have not been verified and they could be explored as well in the near feature.

The speed and position of the target is the essential part of a human monitoring system. The features of RF data mentioned above can not only potentially achieve the goal of occupancy detection but also shall be capable of estimating the speed and the position. The examination of measuring the distances of the human subject via passive wireless signals indoors is being implemented in our lab and the study results will be released soon. The measurement of speed via passive RF data without using specific type of wireless signals has not been conducted or the work has not been issued. So, the investigation into it would be worth of time.

While the question of whether the number of human subjects in the enclosed space can be counted accurately using this method has not been answered. This is also an import aspect of the surveillance system which can draw attention of researchers. Being aware of the quantity of targets, a smarter judgment can be made comparing to such information being absent.

Furthermore, the study of HOD in the open space employing the same methodology illustrated in this research has not been announced by the time when this thesis is issued. It has broad applications such as rescuing lives in the darkness or sight is block by the obstacles during the disasters. The scope of passive RF human HOD system will be extended if the feasibility in the open space is verified.

The intrinsic properties of human body, for example the mass and the size, have not been investigated for HOD yet. These characteristics potentially can be utilized for target differentiation and it will be an extremely attractive feature of such monitoring system. With the ability of discerning the monitoring objects, the defense system would be able to make more responsive decision thus a more intelligent system could be established.

REFERENCES

[1] W. Abd-Almageed, M. Hussein, M. Abdelkader, and L. Davis, “Real-Time Human Detection and Tracking from Mobile Vehicles,” in *2007 IEEE Intelligent Transportation Systems Conference*, Oct. 2007, pp. 149–154.

[2] K. Ikuta, H. Kage, M. Seki, and T. Hirai, “Human intruder detection with Leaky Coaxial cables for wide area surveillance system,” in *2011 IEEE International Conference on Systems, Man, and Cybernetics*, Oct. 2011, pp. 103–108.

[3] J. Watada and Z. B. Musaand, “Tracking human motions for security system,” in *2008 SICE Annual Conference*, Aug. 2008, pp. 3344–3349.

[4] C. Zeng and H. Ma, “Human detection using multi-camera and 3D scene knowledge,” in *2011 18th IEEE International Conference on Image Processing*, Sep. 2011, pp. 1793–1796.

[5] T. Taipalus and J. Ahtiainen, “Human detection and tracking with knee-high mobile 2D LIDAR,” in *2011 IEEE International Conference on Robotics and Biomimetics*, Dec. 2011, pp. 1672–1677.

[6] V. Chen, “Detection and analysis of human motion by radar,” in *2008 IEEE Radar Conference*, May 2008, pp. 1–4.

[7] S. Chang, N. Mitsumoto, and J. W. Burdick, “An algorithm for UWB radar-based human detection,” in *2009 IEEE Radar Conference*, May 2009, pp. 1–6.

[8] H. Kazuhiko, Y. Nobuyuki, and M. Katsuya, “Human occupancy detection method and system for implementing the same,” 5703367, Dec. 1997.

[9] S. Sonia, A. M. Tripathi, R. D. Baruah, and S. B. Nair, “Ultrasonic sensor-based human detector using one-class classifiers,” in *2015 IEEE International Conference on Evolving and Adaptive Intelligent Systems (EAIS)*, Dec. 2015, pp. 1–6.

[10] B. Mrazovac, B. M. Todorović, D. Kukolj, and M. Temerinac, “Device-free human presence detection using frequency domain,” in *2015 IEEE 1st International Workshop on Consumer Electronics (CE WS)*, Mar. 2015, pp. 23–26.

[11] H. Li, C. Wan, R. C. Shah, A. P. Sample, and S. N. Patel, “IDAct: Towards Unobtrusive Recognition of User Presence and Daily Activities,” in *2019 IEEE International Conference on RFID (RFID)*, Apr. 2019, pp. 1–8.

[12] H. Zou, Y. Zhou, J. Yang, and C. J. Spanos, “Towards occupant activity driven smart buildings via WiFi-enabled IoT devices and deep learning,” *Energy and Buildings*, vol. 177, pp. 12–22, Oct. 2018.

[13] S. Lv, Y. Lu, M. Dong, X. Wang, Y. Dou, and W. Zhuang, “Qualitative Action Recognition by Wireless Radio Signals in Human–Machine Systems,” *IEEE Transactions on Human-Machine Systems*, vol. 47, no. 6, Art. no. 6, Dec. 2017.

[14] S. Pan, A. Bonde, J. Jing, L. Zhang, P. Zhang, and H. Y. Noh, “Building Occupancy Estimation System using sparse ambient vibration monitoring,” Apr. 2014, vol. 9061.

[15] P. M. Birch, R. C. D. Young, F. Claret-Tournier, and C. R. Chatwin, “Automated vehicle occupancy monitoring,” *Optical Engineering*, vol. 43, no. 8, pp. 1828–1832, Aug. 2004.

[16] H.-C. Shih, “A robust occupancy detection and tracking algorithm for the automatic monitoring and commissioning of a building,” *Energy and Buildings*, vol. 77, pp. 270–280, Jul. 2014.

[17] W. D. van Eeden, J. P. de Villiers, R. J. Berndt, W. A. J. Nel, and E. Blasch, “Micro-Doppler radar classification of humans and animals in an operational environment,” *Expert Systems with Applications*, vol. 102, pp. 1–11, Jul. 2018.

[18] W. Wang, J. Xiao, Y. Feng, Q. Guo, and L. Wang, “Characteristics of an air source heat pump with novel photoelectric sensors during periodic frost–defrost cycles,” *Applied Thermal Engineering*, vol. 50, no. 1, Art. no. 1, Jan. 2013.

[19] P. Christiansen, K. A. Steen, R. N. Jørgensen, and H. Karstoft, “Automated Detection and Recognition of Wildlife Using Thermal Cameras,” vol. 14, no. 8, Art. no. 8, Jul. 2014.

[20] J. Brokešová, J. Málek, and P. Kolínský, “Rotaphone, a mechanical seismic sensor system for field rotation rate measurements and its in situ calibration,” *Journal of Seismology*, vol. 16, no. 4, Art. no. 4, Oct. 2012.

[21] P. Falcone, F. Colone, A. Macera, and P. Lombardo, “Two-dimensional location of moving targets within local areas using WiFi-based multistatic passive radar,” *IET Radar, Sonar & Navigation*, vol. 8, no. 2, Art. no. 2, Feb. 2014.

[22] M. Kulin, K. Kazaz, I. Moerman, and E. D. Poorter, “End-to-End Learning From Spectrum Data: A Deep Learning Approach for Wireless Signal Identification in Spectrum Monitoring Applications,” *IEEE Access*, vol. 6, pp. 18484–18501, 2018.

[23] T. J. O’Shea, T. Roy, and T. C. Clancy, “Over-the-Air Deep Learning Based Radio Signal Classification,” *IEEE Journal of Selected Topics in Signal Processing*, vol. 12, no. 1, pp. 168–179, Feb. 2018.

[24] S. Riyaz, K. Sankhe, S. Ioannidis, and K. Chowdhury, "Deep Learning Convolutional Neural Networks for Radio Identification," *IEEE Communications Magazine*, vol. 56, no. 9, Art. no. 9, Sep. 2018.

[25] K. Youssef, L. Bouchard, K. Haigh, J. Silovsky, B. Thapa, and C. V. Valk, "Machine Learning Approach to RF Transmitter Identification," *IEEE Journal of Radio Frequency Identification*, vol. 2, no. 4, Art. no. 4, Dec. 2018.

[26] D. Roy, T. Mukherjee, M. Chatterjee, and E. Pasiliao, "Detection of Rogue RF Transmitters using Generative Adversarial Nets," in *2019 IEEE Wireless Communications and Networking Conference (WCNC)*, Apr. 2019, pp. 1–7.

[27] M. Zhao *et al.*, "Through-Wall Human Pose Estimation Using Radio Signals," in *2018 IEEE/CVF Conference on Computer Vision and Pattern Recognition*, Jun. 2018, pp. 7356–7365.

[28] Y. Tian, G.-H. Lee, H. He, C.-Y. Hsu, and D. Katabi, "RF-Based Fall Monitoring Using Convolutional Neural Networks," *Proc. ACM Interact. Mob. Wearable Ubiquitous Technol.*, vol. 2, no. 3, Sep. 2018.

[29] M. Edrich and A. Schroeder, "Multiband multistatic Passive Radar system for airspace surveillance: A step towards mature PCL implementations," in *2013 International Conference on Radar*, Sep. 2013, pp. 218–223.

[30] S. Wang and G. Zhou, "A review on radio based activity recognition," *Digital Communications and Networks*, vol. 1, no. 1, pp. 20–29, 2015.

[31] K. Vasudeva, B. S. Çiftler, A. Altamar, and I. Guvenc, "An experimental study on RSS-based wireless localization with software defined radio," in *WAMICON 2014*, Jun. 2014, pp. 1–6.

[32] J. Bonior, Z. Hu, T. N. Guo, R. C. Qiu, J. P. Browning, and M. C. Wicks, "Software-Defined-Radio-Based Wireless Tomography: Experimental Demonstration and Verification," *IEEE Geoscience and Remote Sensing Letters*, vol. 12, no. 1, Art. no. 1, Jan. 2015.

[33] T. Zhang, T. Song, D. Chen, T. Zhang, and J. Zhuang, "A Wifi-Based Gesture Recognition System Using Software-Defined Radio," *IEEE Access*, vol. 7, pp. 131102–131113, 2019.

[34] F. K. Jondral, "Software-Defined Radio—Basics and Evolution to Cognitive Radio," *EURASIP Journal on Wireless Communications and Networking*, vol. 2005, no. 3, Art. no. 3, Aug. 2005.

[35] B. Wang and K. J. R. Liu, “Advances in cognitive radio networks: A survey,” *IEEE Journal of Selected Topics in Signal Processing*, vol. 5, no. 1, Art. no. 1, Feb. 2011.

[36] G. Wang, K. Pham, E. Blasch, T. M. Nguyen, D. Shen, and X. Tian, “Cognitive radio unified Spectral efficiency and Energy Efficiency trade-off analysis,” in *MILCOM 2015 - 2015 IEEE Military Communications Conference*, Oct. 2015, pp. 244–249.

[37] X. Liu and X. Zhang, “NOMA-Based Resource Allocation for Cluster-Based Cognitive Industrial Internet of Things,” *IEEE Transactions on Industrial Informatics*, vol. 16, no. 8, Art. no. 8, Aug. 2020.

[38] Y. Shi, K. Davaslioglu, Y. Sagduyu, W. Headley, M. Fowler, and G. Green, *Deep Learning for RF Signal Classification in Unknown and Dynamic Spectrum Environments*. 2019, p. 10.

[39] V. K. Tumuluru, P. Wang, and D. Niyato, “Channel Status Prediction for Cognitive Radio Networks,” *Wirel. Commun. Mob. Comput.*, vol. 12, no. 10, Art. no. 10, Jul. 2012.

[40] Y. Lin, C. Wang, J. Wang, and Z. Duo, “A Novel Dynamic Spectrum Access Framework Based on Reinforcement Learning for Cognitive Radio Sensor Networks,” *Sensors*, vol. 16, no. 10, Art. no. 10, 2016.

[41] R. Ranganathan *et al.*, “Cognitive Radio for Smart Grid: Theory, Algorithms, and Security,” *International Journal of Digital Multimedia Broadcasting*, vol. 2011, p. 502087, Jun. 2011.

[42] G. P. Joshi, S. Y. Nam, and S. W. Kim, “Cognitive Radio Wireless Sensor Networks: Applications, Challenges and Research Trends,” *Sensors (Basel, Switzerland)*, vol. 13, pp. 11196–228, Sep. 2013.

[43] U. K. Majumder, E. P. Blasch, and D. A. Garren, *Deep Learning for Radar and Communications Automatic Target Recognition*. Artech House, 2020.

[44] G. Vanhoy, N. Teku, and T. Bose, “Feature selection for cyclostationary-based signal classification,” *Proceedings of the International Telemetering Conference*, Jan. 2017.

[45] X. Wang, Y. Zhang, H. Zhang, X. Wei, and G. Wang, “Identification and authentication for wireless transmission security based on RF-DNA fingerprint,” *EURASIP Journal on Wireless Communications and Networking*, vol. 2019, no. 1, Art. no. 1, Sep. 2019.

[46] C. E. Galván-Tejada, J. P. García-Vázquez, and R. F. Brena, “Magnetic Field Feature Extraction and Selection for Indoor Location Estimation,” *Sensors*, vol. 14, no. 6, Art. no. 6, 2014.

[47] D. Roy, T. Mukherjee, M. Chatterjee, E. Blasch, and E. Pasiliao, “RFAL: Adversarial Learning for RF Transmitter Identification and Classification,” *IEEE Transactions on Cognitive Communications and Networking*, vol. 6, no. 2, pp. 783–801, Jun. 2020.

[48] I. J. Goodfellow *et al.*, *Generative Adversarial Networks*. 2014.

[49] D. N. Tran, T. D. Tran, and L. Nguyen, “Generative adversarial networks for recovering missing spectral information,” in *2018 IEEE Radar Conference (RadarConf18)*, Apr. 2018, pp. 1223–1227.

[50] Z. Li, J. Cao, H. Wang, and M. Zhao, “Sparsely Self-Supervised Generative Adversarial Nets for Radio Frequency Estimation,” *IEEE Journal on Selected Areas in Communications*, vol. 37, no. 11, Art. no. 11, 2019.

[51] X. Liu and X. Wang, “Real-Time Indoor Localization for Smartphones Using Tensor-Generative Adversarial Nets,” *IEEE Transactions on Neural Networks and Learning Systems*, pp. 1–11, 2020.

[52] C. Wu, Y. Wang, and Z. Yin, “Energy-efficiency opportunistic spectrum allocation in cognitive wireless sensor network,” *EURASIP Journal on Wireless Communications and Networking*, vol. 2018, no. 1, p. 13, Jan. 2018.

[53] X. Song, C. Yin, D. Liu, and R. Zhang, “Spatial Throughput Characterization in Cognitive Radio Networks with Threshold-Based Opportunistic Spectrum Access,” *IEEE Journal on Selected Areas in Communications*, vol. 32, no. 11, pp. 2190–2204, Nov. 2014.

[54] Y. Xu, J. Wang, Q. Wu, A. Anpalagan, and Y. Yao, “Opportunistic Spectrum Access in Cognitive Radio Networks: Global Optimization Using Local Interaction Games,” *IEEE Journal of Selected Topics in Signal Processing*, vol. 6, no. 2, Art. no. 2, Apr. 2012.

[55] U. K. Majumder, E. P. Blasch, and D. A. Garren, *Deep Learning for Radar and Communications Automatic Target Recognition*. Artech House, 2020.

[56] B. Kahler and E. Blasch, “Decision-Level Fusion Performance Improvement From Enhanced HRR Radar Clutter Suppression,” Jan. 2011.

[57] J. Hall, M. Barbeau, and E. Kranakis, "Enhancing Intrusion Detection in Wireless Networks using Radio Frequency Fingerprinting," presented at the Communications, Internet, and Information Technology, US, 2004.

[58] M. E. Tipping and C. M. Bishop, "Mixtures of Probabilistic Principal Component Analyzers," *Neural Comput.*, vol. 11, no. 2, pp. 443–482, Feb. 1999.

[59] G. P. McCabe, "Principal Variables," *Technometrics*, vol. 26, no. 2, pp. 137–144, May 1984.

[60] C. Zhang, Y. Li, Z. Yu, and F. Tian, "Feature selection of power system transient stability assessment based on random forest and recursive feature elimination," in *2016 IEEE PES Asia-Pacific Power and Energy Engineering Conference (APPEEC)*, Oct. 2016, pp. 1264–1268.

[61] E. Maby, R. Le Bouquin Jeannes, C. Liegeok-Chauvel, B. Gourevitch, and G. Faucon, "Analysis of auditory evoked potential parameters in the presence of radiofrequency fields using a support vector machines method," *Medical and Biological Engineering and Computing*, vol. 42, no. 4, pp. 562–568, Jul. 2004.

[62] C. Zhu, R. H. Byrd, P. Lu, and J. Nocedal, "Algorithm 778: L-BFGS-B: Fortran Subroutines for Large-Scale Bound-Constrained Optimization," *ACM Trans. Math. Softw.*, vol. 23, no. 4, pp. 550–560, Dec. 1997.

[63] G. P. McCabe, "Principal Variables," *Technometrics*, vol. 26, no. 2, Art. no. 2, May 1984.

[64] I. J. Goodfellow *et al.*, *Generative Adversarial Networks*. 2014.